
IX.
The TeV Sky and
Multiwavelength Astrophysics

Astroparticle Physics a.a. 2021/22

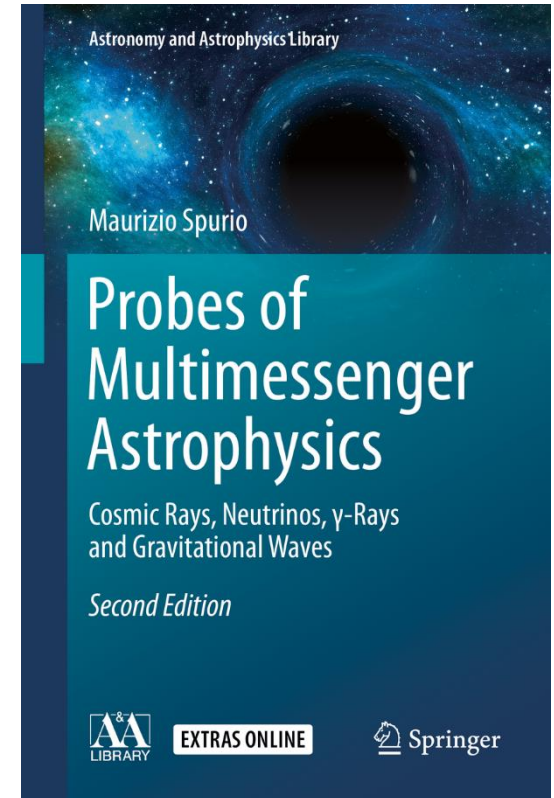
Maurizio Spurio

Università di Bologna e INFN

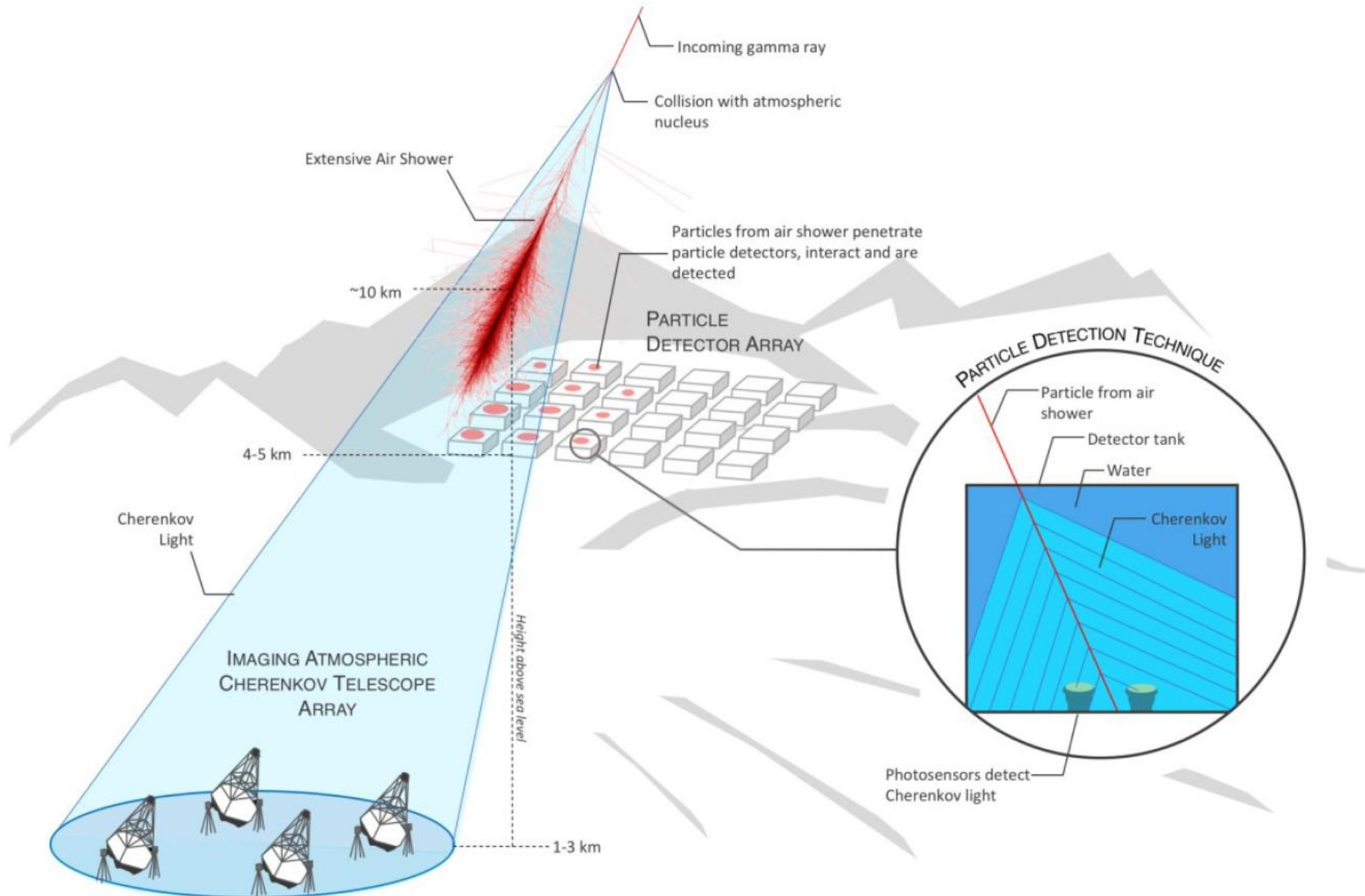
maurizio.spurio@unibo.it

Content

9	The TeV Sky and Multiwavelength Astrophysics
9.1	The Imaging Cherenkov Technique
9.1.1	Gamma-Ray Versus Charged CR Discrimination
9.1.2	HESS, VERITAS and MAGIC
9.2	EAS Arrays for γ -astronomy
9.3	TeV Astronomy: The Catalog
9.4	Gamma-Rays from Pulsars
9.5	The CRAB Pulsar and Nebula
9.6	The Problem of the Identification of Galactic CR Sources
9.7	Extended Supernova Remnants
9.8	The SED of Some Peculiar SNRs
9.9	Summary of the Study of Galactic Accelerators
9.10	Active Galaxies
9.11	The Extragalactic γ -ray Sky
9.12	The Spectral Energy Distributions of Blazars
9.12.1	Quasi-Simultaneous SEDs of Fermi-LAT Blazars
9.12.2	Simultaneous SED Campaigns and Mrk 421
9.13	Jets in Astrophysics
9.13.1	Time Variability in Jets
9.14	The Extragalactic Background Light
	References



Detecting γ -rays on ground: two methods



Ground based detectors for VHE gamma ray

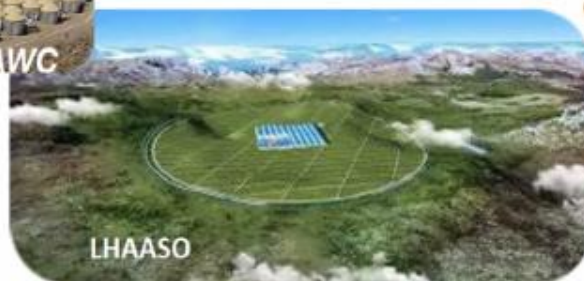
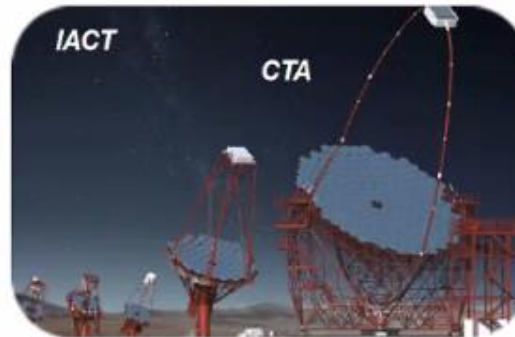
Gamma rays astronomy at energies of TeV is outside the possibility of space-based experiment
 VHE (100 GeV-100TeV) gamma rays can only be studied by means of ground based detector

Two separate methods measure indirectly VHE gamma rays.

- Surface arrays of particle detectors
- Imaging Atmospheric Cherenkov Telescopes (IACTs)

Cherenkov Atmospheric Telescopes


- 20% duty-cycle
- Pointing (few degrees FoV)
- Energy threshold down to 10s GeV
- Good energy and angular resolution



Particle Detector Arrays

- 100% duty-cycle
- Wide-field of View (~ steradian)
- Energy range 100s GeV up to 100s TeV
- Long exposure and accurate background determination

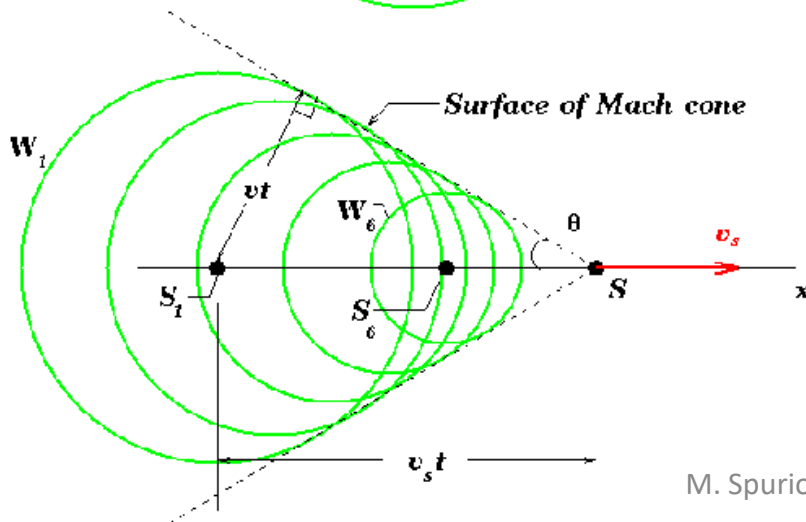
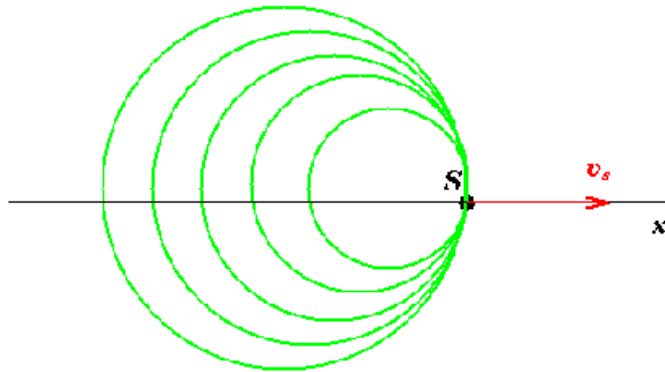
Detecting γ -rays on ground: the Cherenkov technique

- The Earth's atmosphere is opaque to high-energy γ -rays ($X_0 \sim 40 \text{ gcm}^{-2}$) $\rightarrow e^+e^-$
- **Charged particles at ground can be measured with detectors**; the main task is the discrimination between CR-induced and γ -ray induced showers.
- Secondary charged particle in the shower produces **Cherenkov light** at the Cherenkov angle θ , with $\cos\theta = 1/\beta n$, if its velocity exceeds the threshold $\beta=v/c > n$ (Chap. 11) 
- Thus, γ -ray induced showers can be detected also with Cherenkov telescopes.
- As $n \sim 1$ in air, the Cherenkov angle is small (from 0.66° to 0.74°): this results in a focusing of light onto the ground into a ring-like region with typically $R \sim 120 \text{ m}$.
- Atmospheric Cherenkov detectors are of 2 types: **sampling** and **imaging** telescopes. The latter relies on the detection on the ground of the images of the Cherenkov light.
- From the measurement, it is determined the **longitudinal** and **lateral** development of the EM showers \rightarrow the arrival direction and energy of the primary γ -rays.
- Imaging Cherenkov are essentially wide-field optical telescopes consisting of a large reflector of about 10m radius, reflecting the light (the image) into a high-speed multi-PMT camera in the focal plane.
- Short exposures (less than 30 ns) are required to detect the faint flashes of Cherenkov light against the Poisson fluctuation in the night-sky background.

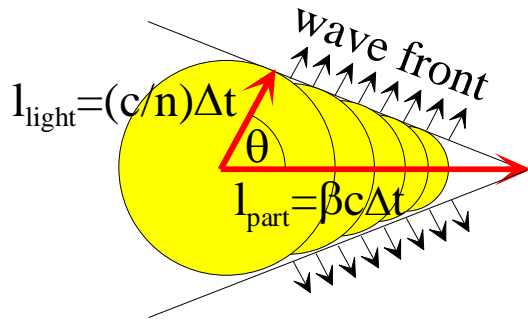
Cherenkov Radiation



- As a charged particle travels, it disrupts the local electromagnetic field (EM) in a medium.
- Electrons in the atoms of the medium will be displaced and polarized by the passing EM field of a charged particle.
- Photons are emitted as an insulator's electrons restore themselves to equilibrium after the disruption has passed.
- In a conductor, the EM disruption can be restored without emitting a photon.
- In normal circumstances, these photons destructively interfere with each other and no radiation is detected.
- However, when the disruption travels faster than light is propagating through the medium, the photons constructively interfere and intensify the observed Cherenkov radiation.

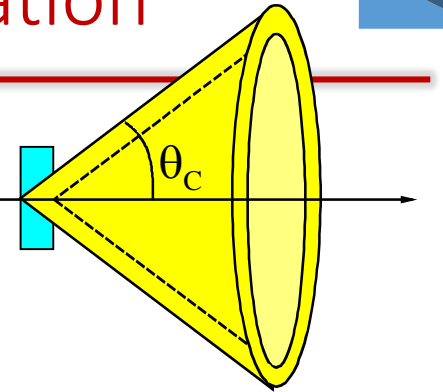


Cherenkov Radiation



$$\cos \theta_c = \frac{1}{n\beta}$$

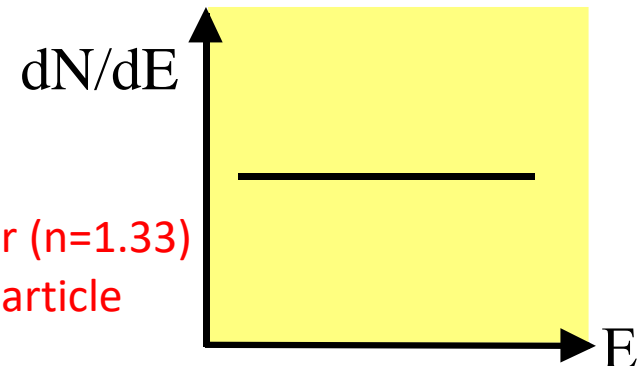
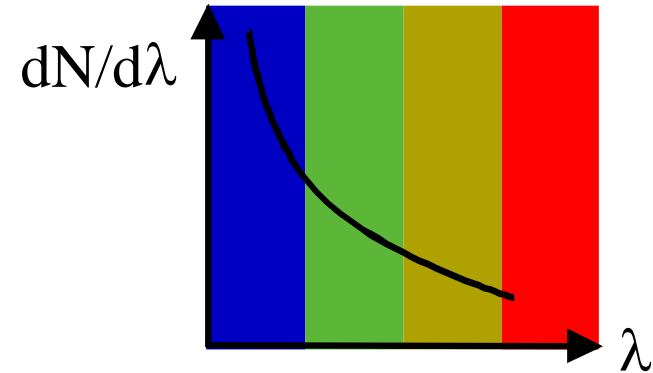
with $n = n(\lambda) \geq 1$



- Threshold velocity $\beta_T = 1/n \rightarrow \theta_T \sim 0$
- Angle of emission ($\beta=1$): $\theta_{\max} = \arccos(1/n)$
- Distribution of emitted photons:

$$\frac{d^2 N}{dx d\lambda} = \frac{2\pi z^2 \alpha}{\lambda^2} \left(1 - \frac{1}{\beta^2 n^2} \right) = \frac{2\pi \cdot z^2 \alpha}{\lambda^2} \sin^2 \theta_c$$

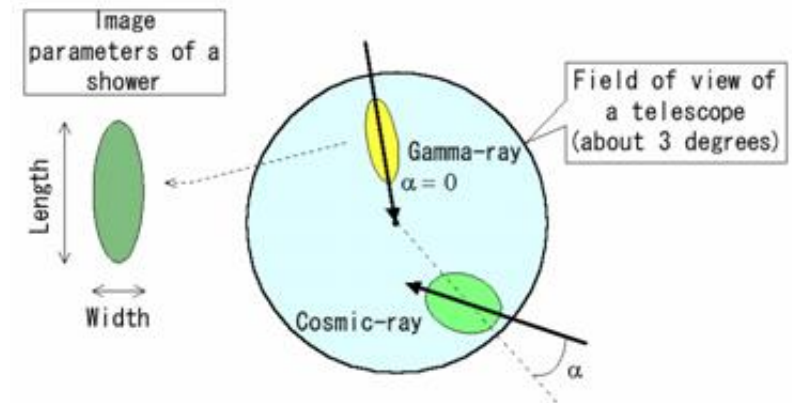
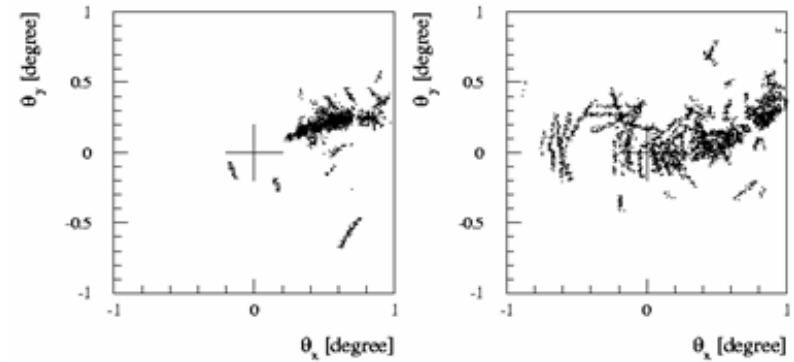
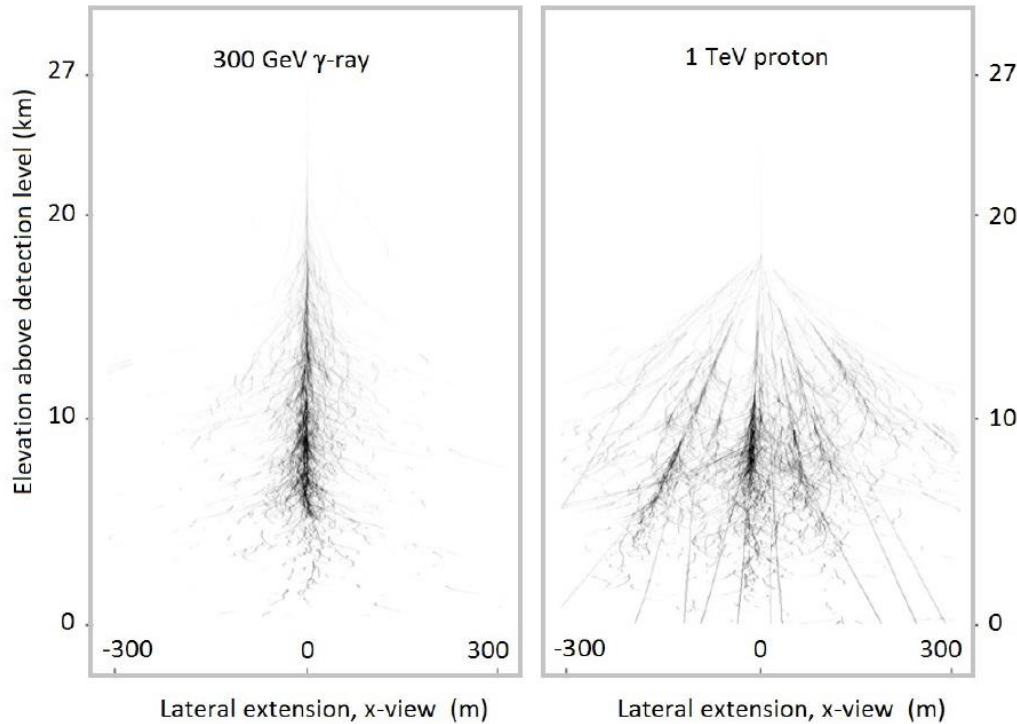
$$\frac{d^2 N}{dx dE} = \frac{z^2 \alpha}{\hbar c} \sin^2 \theta_c$$

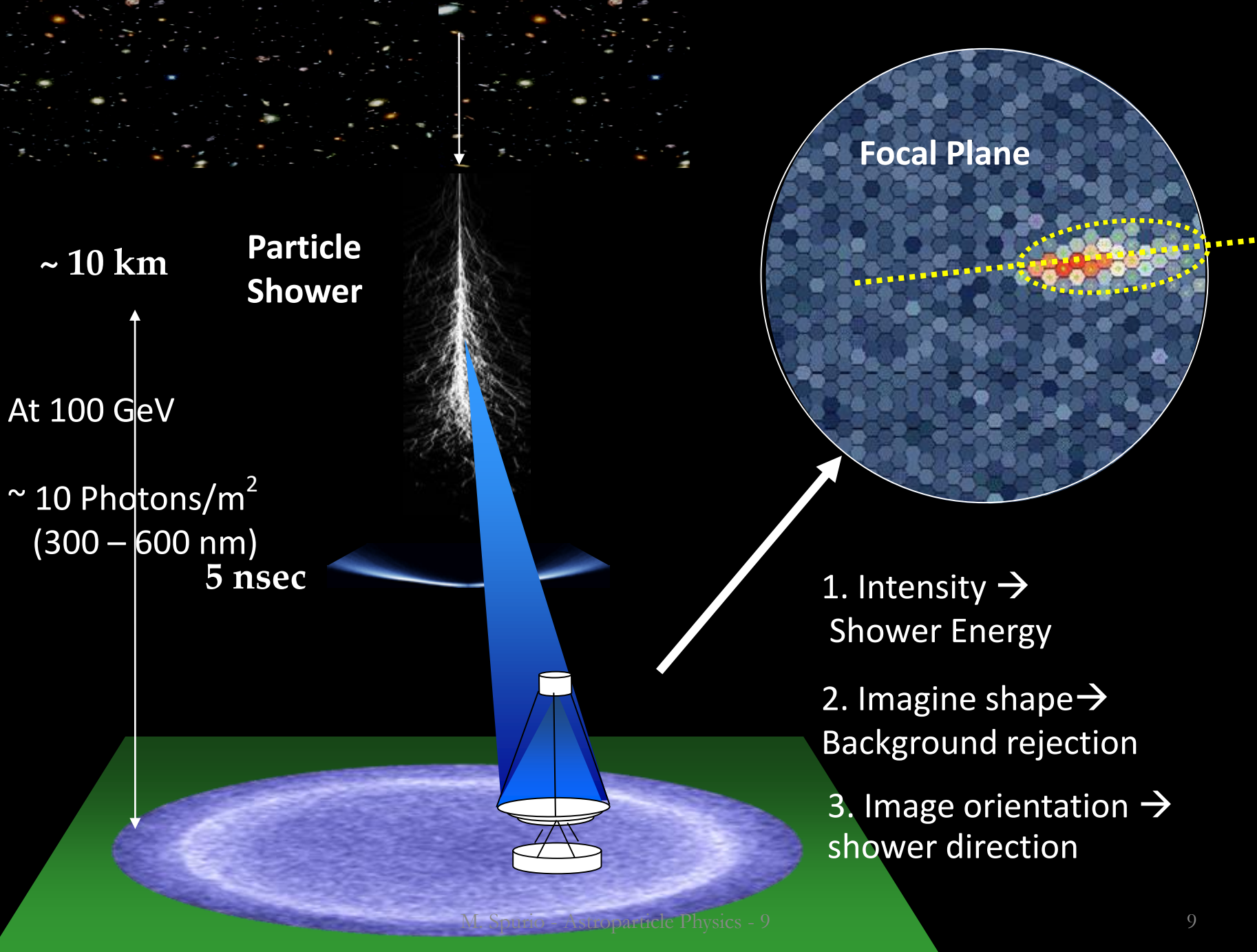


Question: Evaluate the number of Cherenkov photons in water ($n=1.33$) in the $\lambda=300-600$ nm interval for a relativistic single charged particle

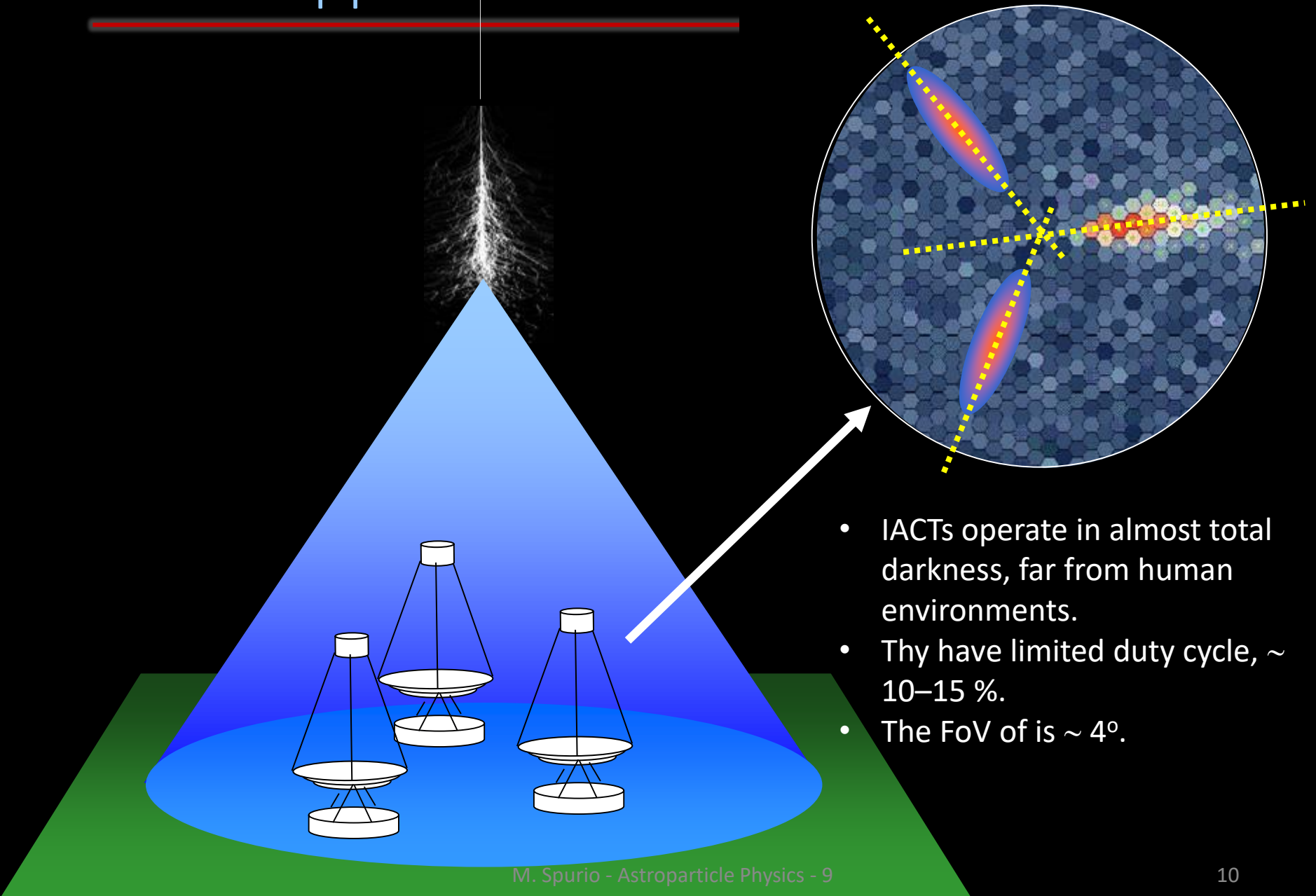
Charged CR rejection

Comparison of a pure EM shower (from a 300 GeV γ -ray) and a shower initiated by a 1 TeV proton. The plot shows the projection of secondary particle trajectories onto a plane in which the ordinate corresponds to the elevation



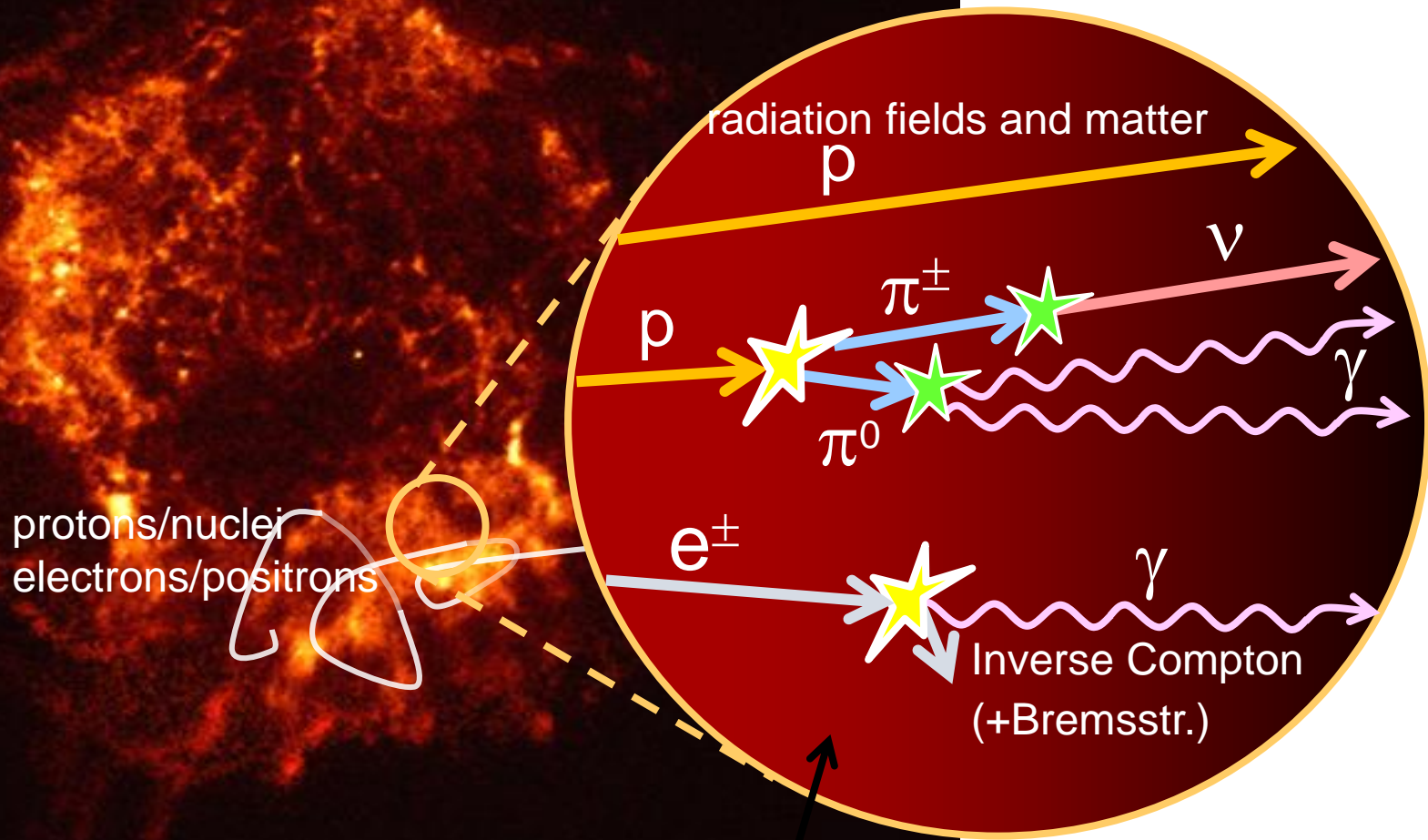


Stereo Approach



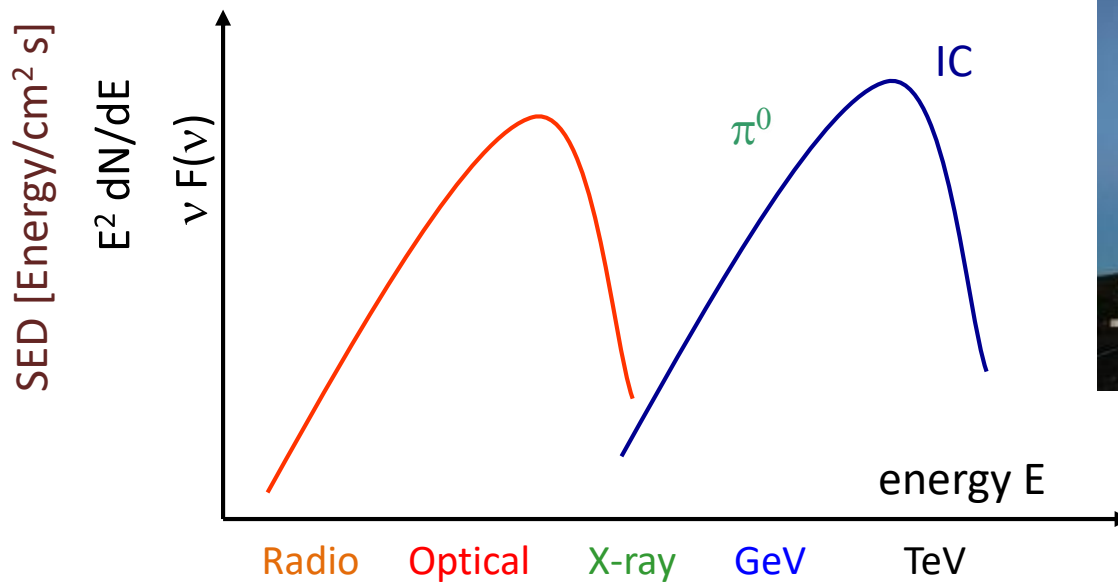
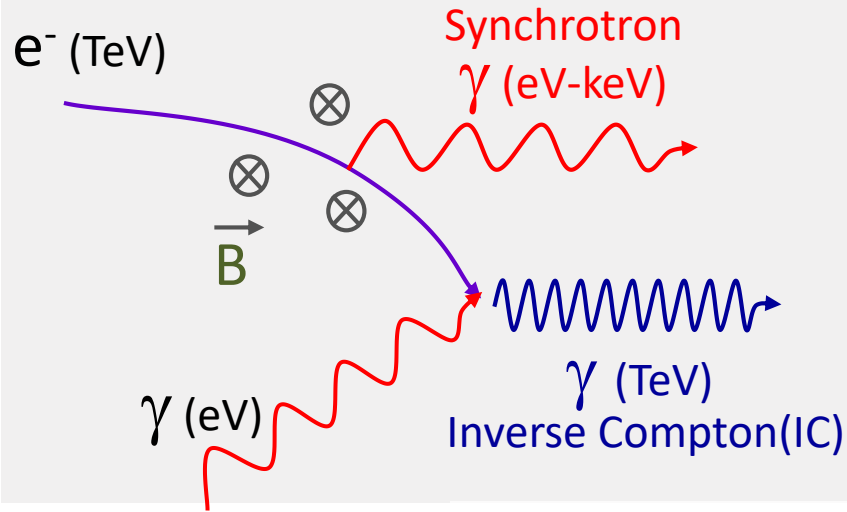
- IACTs operate in almost total darkness, far from human environments.
- They have limited duty cycle, $\sim 10\text{--}15\%$.
- The FoV of is $\sim 4^\circ$.

CRs and Secondary neutral particles@sources



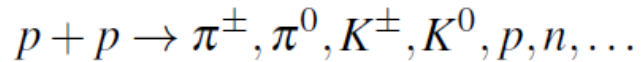
Non-thermal Universe: leptonic model

leptonic processes

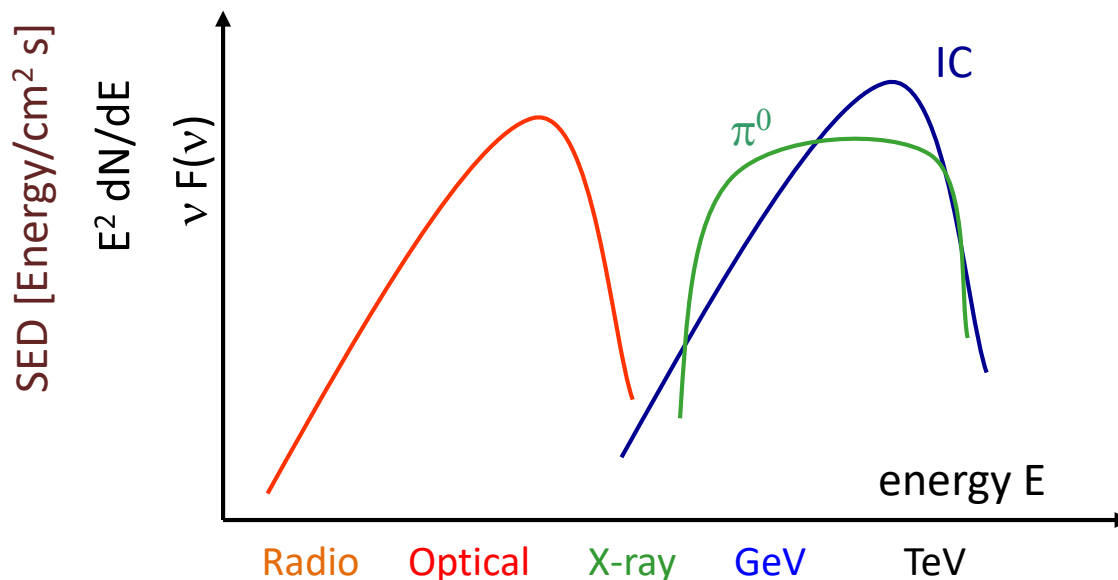
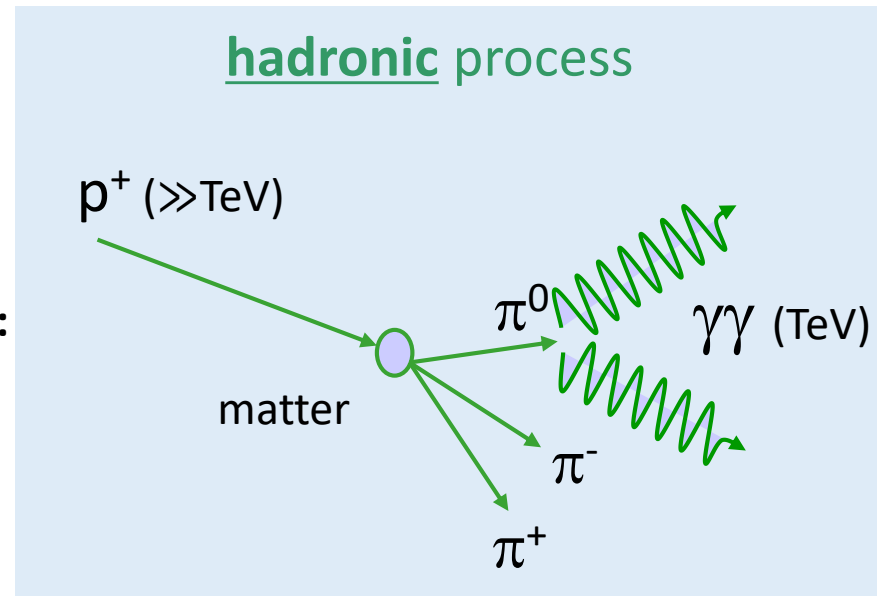
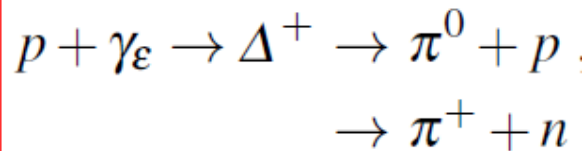


Non-thermal Universe: hadronic model

1) Astrophysical beam dump mechanism.

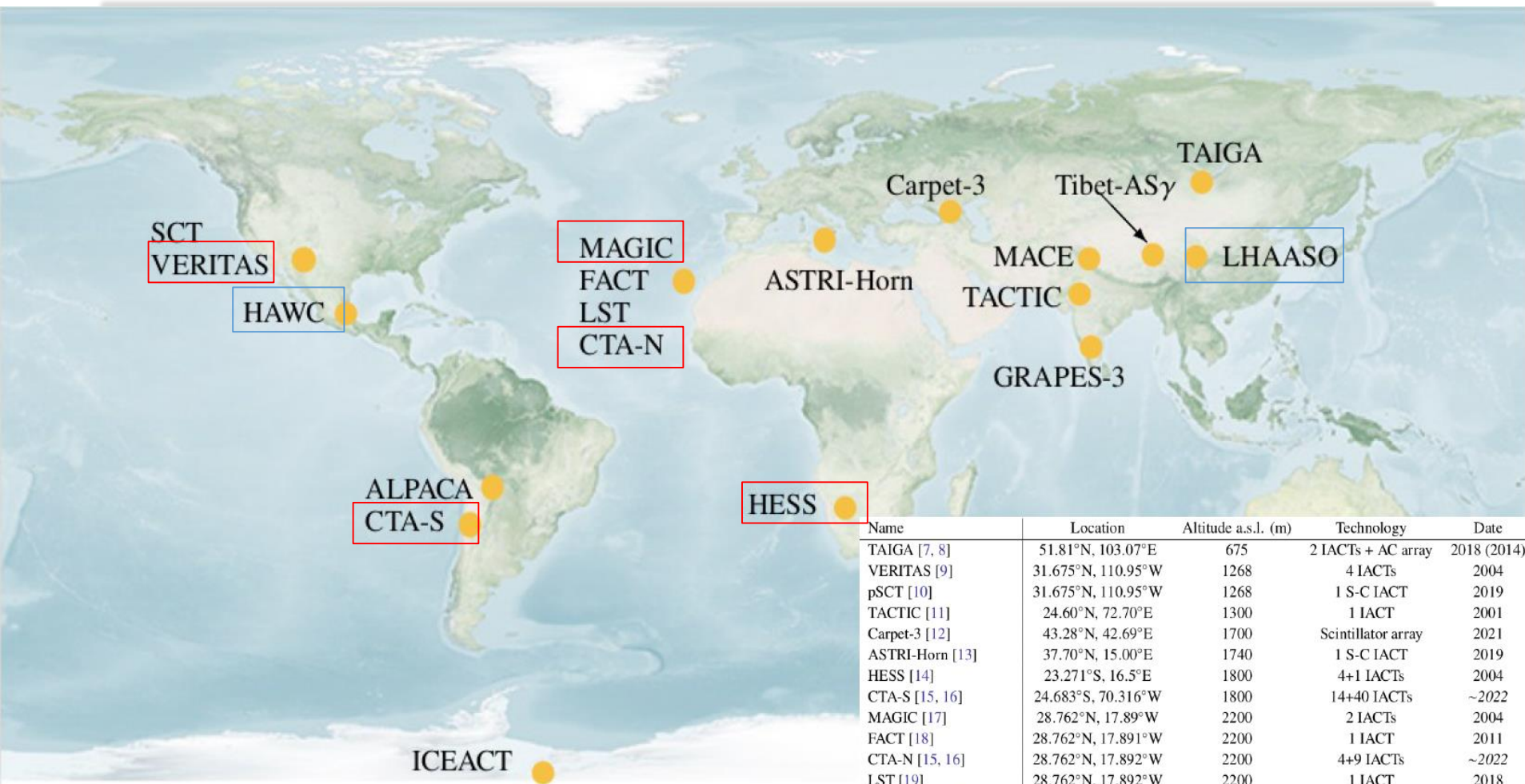


2) Photoproduction through the Δ^+ resonance:



To distinguish between **hadronic/leptonic** origin the **Spectral Energy Distribution (SED)** must be studied with different experimental techniques.

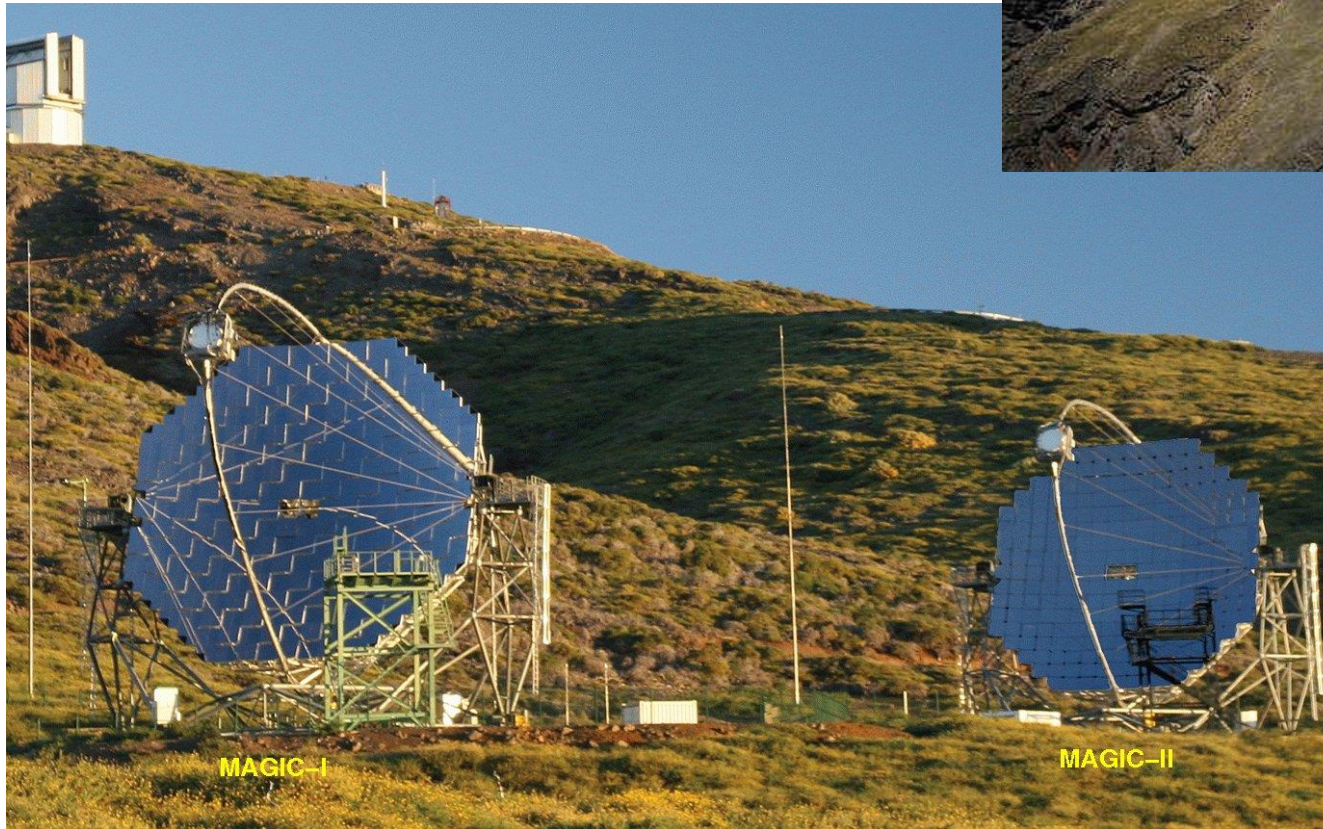
Distribution of IACTs on Earth



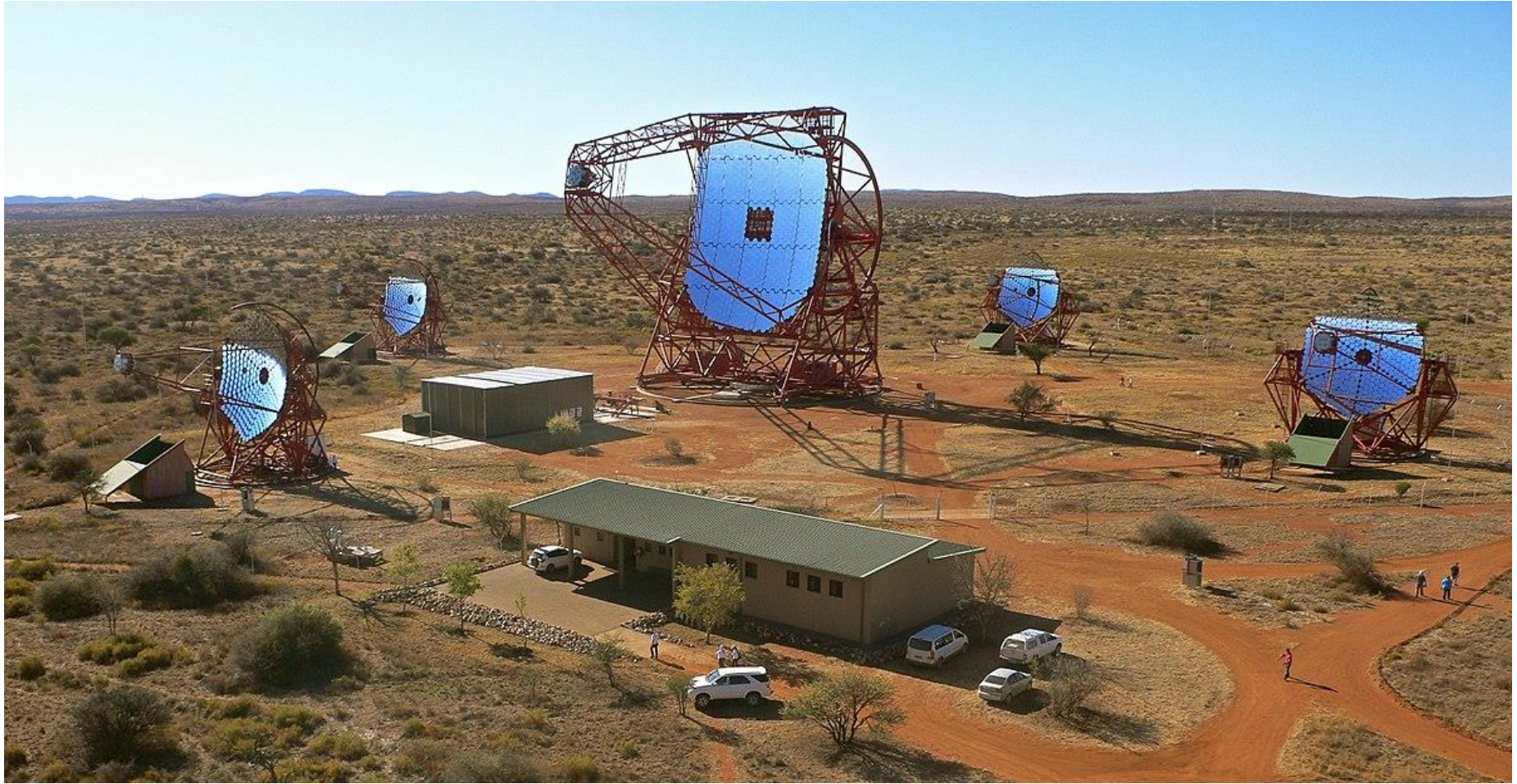
Name	Location	Altitude a.s.l. (m)	Technology	Date
TAIGA [7, 8]	51.81°N, 103.07°E	675	2 IACTs + AC array	2018 (2014)
VERITAS [9]	31.675°N, 110.95°W	1268	4 IACTs	2004
pSCT [10]	31.675°N, 110.95°W	1268	1 S-C IACT	2019
TACTIC [11]	24.60°N, 72.70°E	1300	1 IACT	2001
Carpet-3 [12]	43.28°N, 42.69°E	1700	Scintillator array	2021
ASTRI-Horn [13]	37.70°N, 15.00°E	1740	1 S-C IACT	2019
HESS [14]	23.271°S, 16.5°E	1800	4+1 IACTs	2004
CTA-S [15, 16]	24.683°S, 70.316°W	1800	14+40 IACTs	~2022
MAGIC [17]	28.762°N, 17.89°W	2200	2 IACTs	2004
FACT [18]	28.762°N, 17.891°W	2200	1 IACT	2011
CTA-N [15, 16]	28.762°N, 17.892°W	2200	4+9 IACTs	~2022
LST [19]	28.762°N, 17.892°W	2200	1 IACT	2018
GRAPES-3 [20]	11.39°N, 76.66°E	2200	Scintillator array	2000
IceACT [21]	89.99°S, 63.453°W	2840	2 ACT	2019
HAWC [22]	18.995°N, 97.309°W	4100	300+345 WCDs	2013
MACE [23]	32.78°N, 78.96°E	4270	1 IACT	2020
Tibet-ASy [24]	30.11°N, 90.53°E	4300	Scintillators+WCDs	2014 [†]
LHAASO [25]	29.359°N, 100.138°E	4410	Scintillators+WCDs	2018
ALPACA [26]	16.383°S, 68.133°W	4740	Scintillator array	2017*
ASTRI [27]	38.30°N, 14.51°W	2200	1 S-C IACT	2022

MAGIC at La Palma

- The largest reflector in the world (2 x 17 meters diameter telescopes)
- International collaboration of 160 scientists from Germany, Italy, Spain, Japan, Croatia, Switzerland, Finland, Poland, Bulgaria



The HESS telescope (Nanibia)



VERITAS in Utah



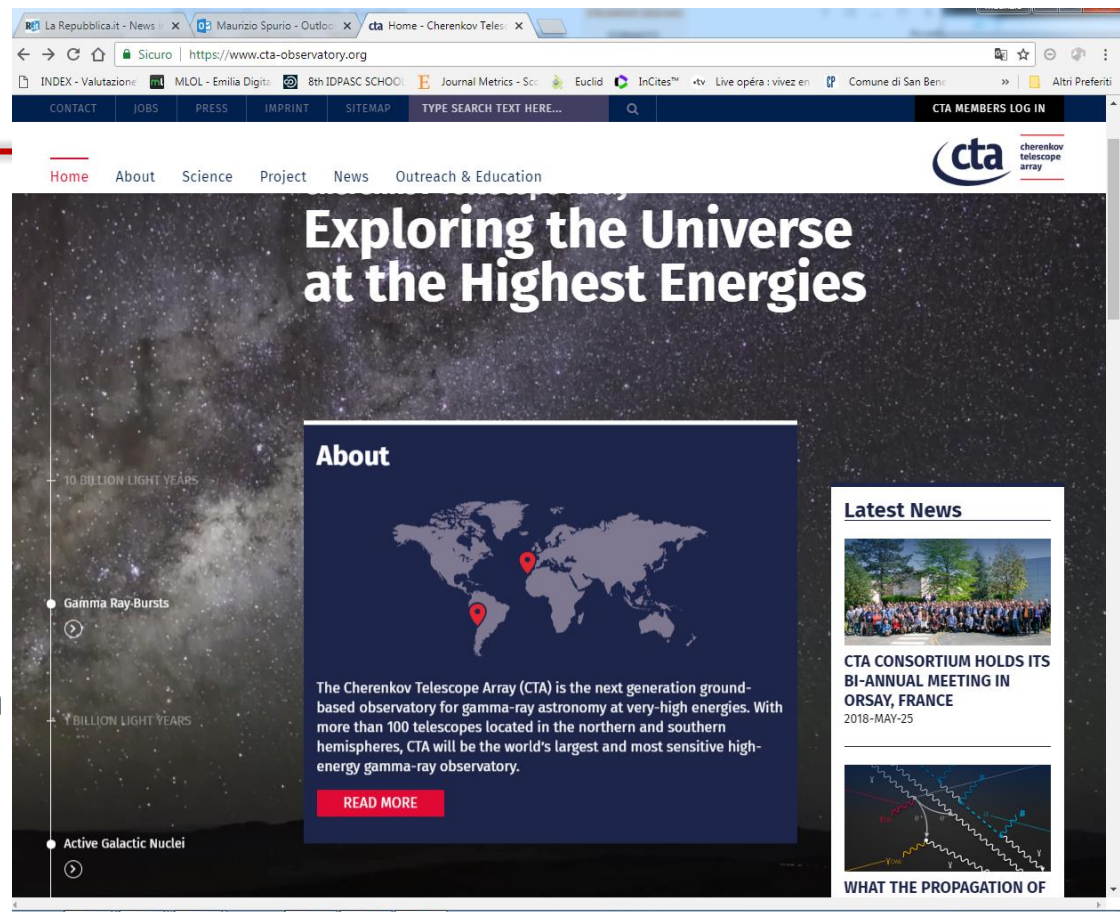
Comparison among IACTs

Instr.	Tels. #	Tel. A (m ²)	FoV (°)	Tot A (m ²)	Thresh. (TeV)	PSF (°)	Sens. (%Crab)
H.E.S.S.	4	107	5	428	0.1	0.06	0.7
MAGIC	2	236	3.5	472	0.05(0.03)	0.06	0.8
VERITAS	4	106	4	424	0.1	0.07	0.7

The future: CTA

<https://www.cta-observatory.org/>

CTA will be the largest ground-based γ -ray detection observatory in the world, with more than 100 telescopes in the **Northern** (Canarias' IAC's) and **Southern** (Paranal Observatory in the Atacama Desert, Chile) hemispheres



The screenshot shows the homepage of the Cherenkov Telescope Array (CTA) website. The main heading is "Exploring the Universe at the Highest Energies". Below this, there is an "About" section with a world map showing the locations of the Northern and Southern observatories. The text describes CTA as the next generation ground-based observatory for gamma-ray astronomy, consisting of more than 100 telescopes. A "READ MORE" button is visible. To the right, there is a "Latest News" section with a photo of a meeting and the title "CTA CONSORTIUM HOLDS ITS BI-ANNUAL MEETING IN ORSAY, FRANCE".



Bologna as the host site of the CTA Headquarters

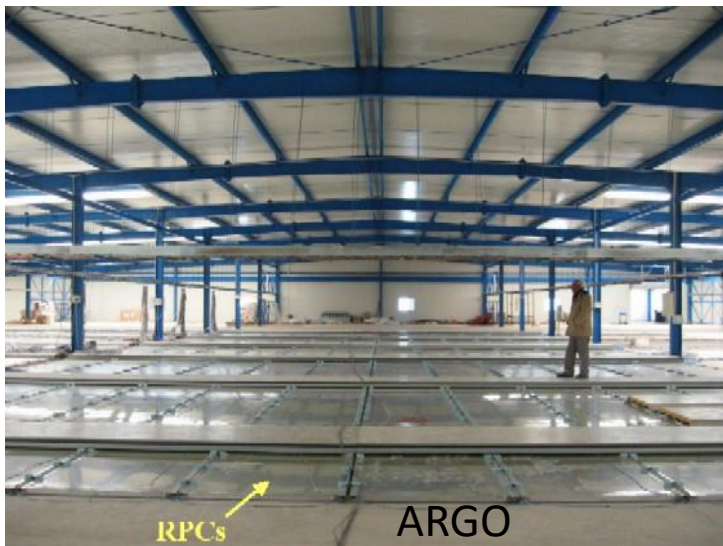
Munich, Germany – On 13 June 2016, the governing body of the Cherenkov Telescope Array Observatory gGmbH (CTAO gGmbH), the CTA Council, **selected Bologna as the host site of the CTA Headquarters** and Berlin - Zeuthen for the Science Data Management Centre (SDMC) from five site candidates.



<https://www.cta-observatory.org/headquarters-science-data-management-centre-sites-selected/>

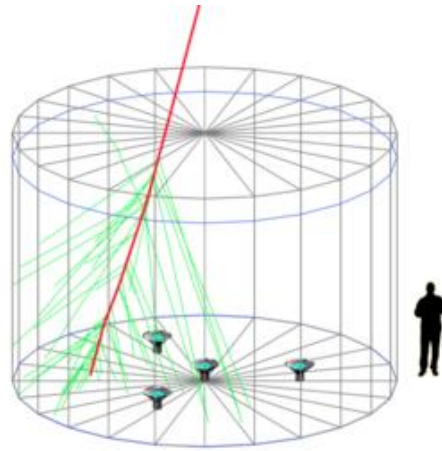
EAS Arrays for γ -astronomy

- The EAS technique, designed for the detection of CRs at PeV -EeV energies, can also be adopted for γ -ray astronomy.
- The mandatory requirement is that the energy threshold be reduced to the $>TeV$ scale using dense particle arrays located at very high altitudes.
- The feasibility of the measurement at ground level of showers initiated by a γ -ray has been successfully demonstrated by the Milagro (2000 to 2008 in New Mexico) and ARGO (Tibet, 2001-2013) Collaborations

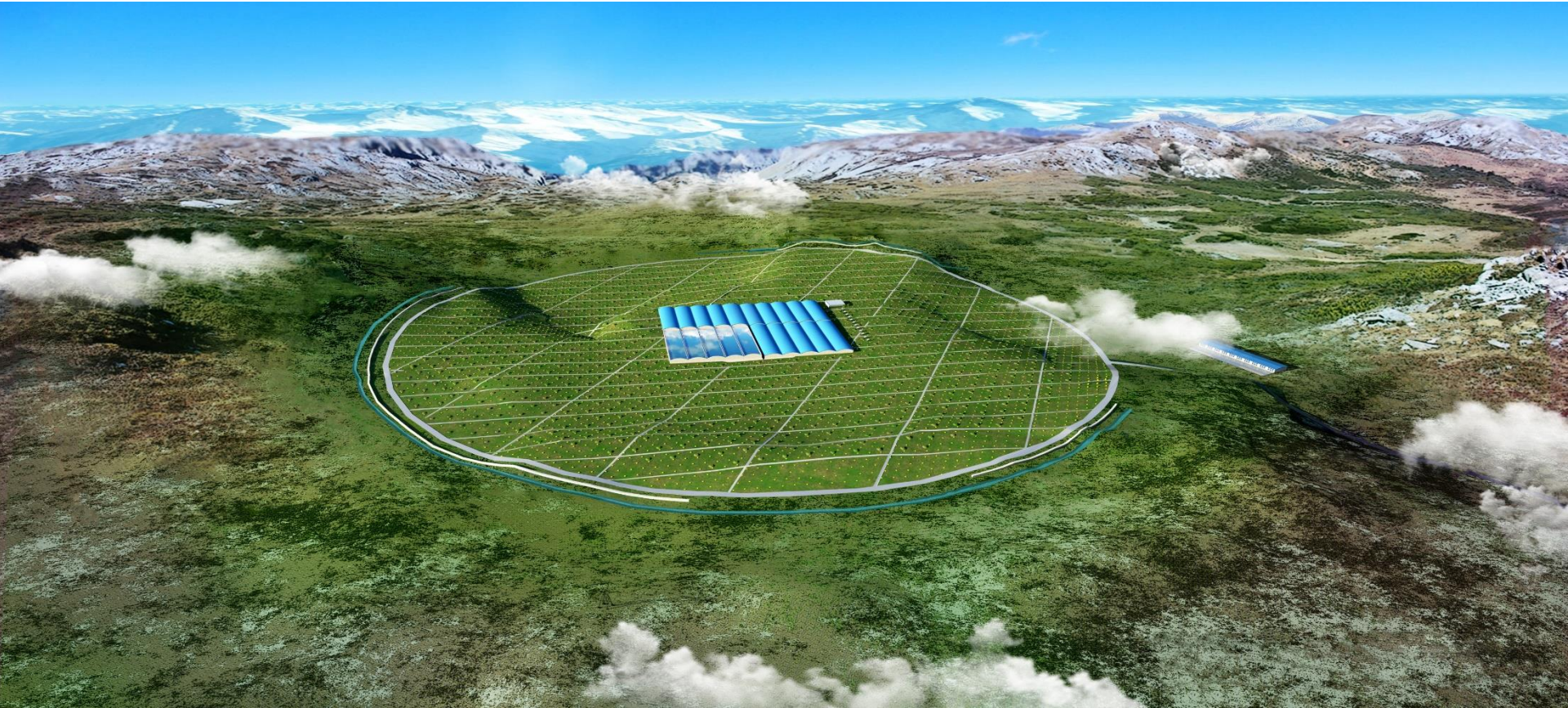


HAWC in Mexico

- HAWC was completed in 2015, located at 4,100m close to Sierra Negra, Mexico.
- it consists of an array of 300 water Cherenkov detectors.



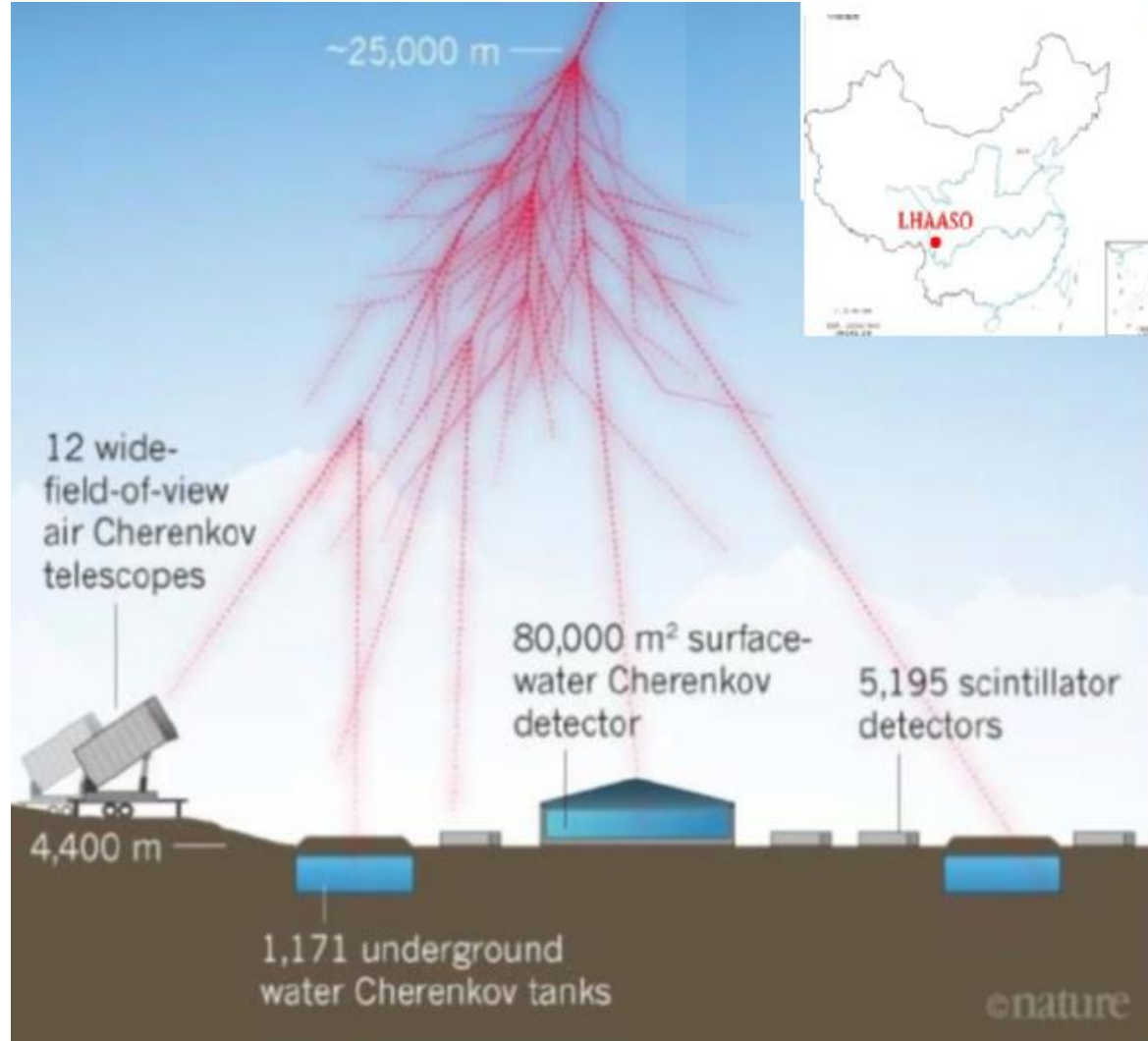
LHAASO in China (start 2020)



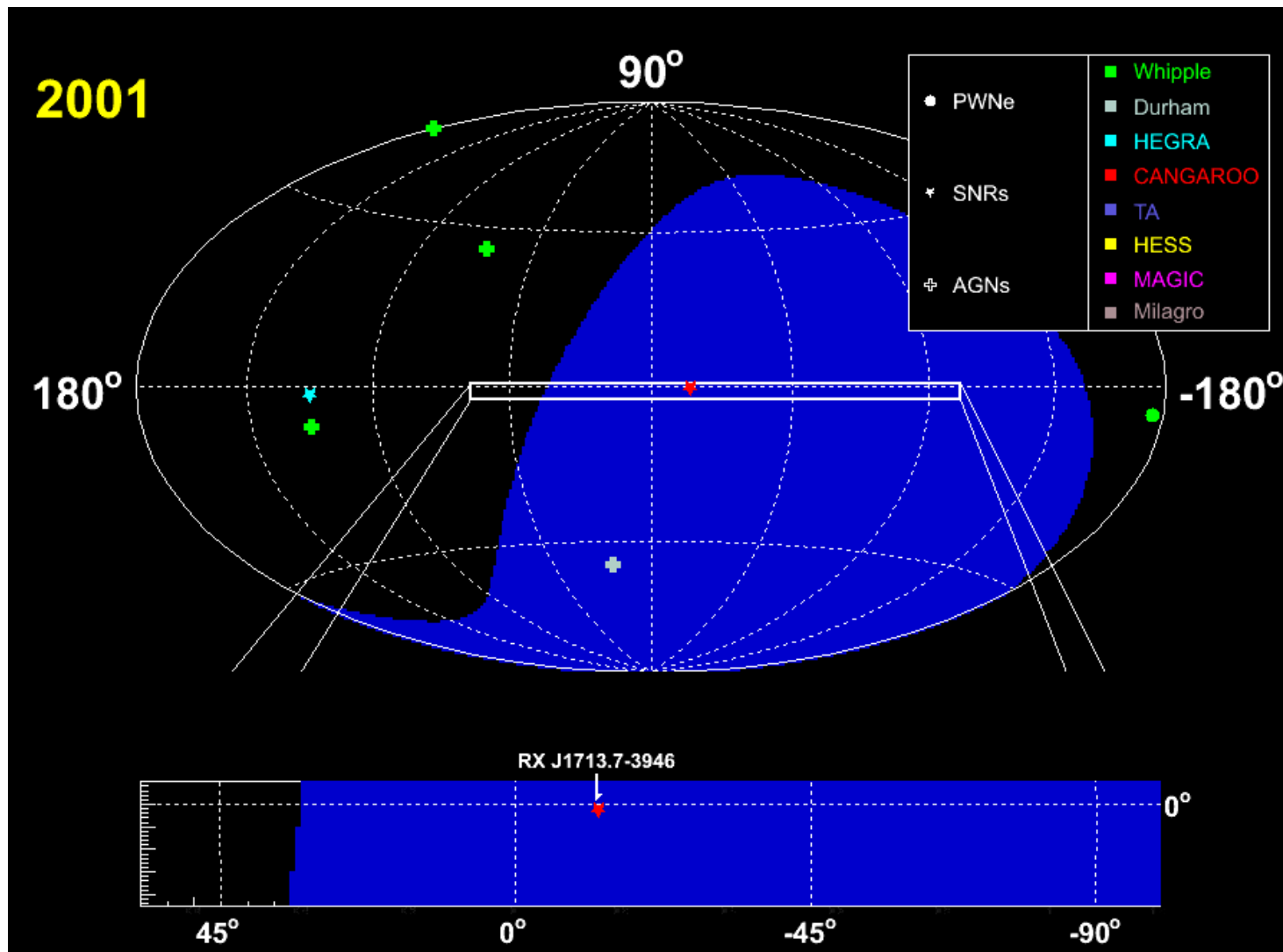
LHAASO in China (start 2020)

Three different kind of instruments

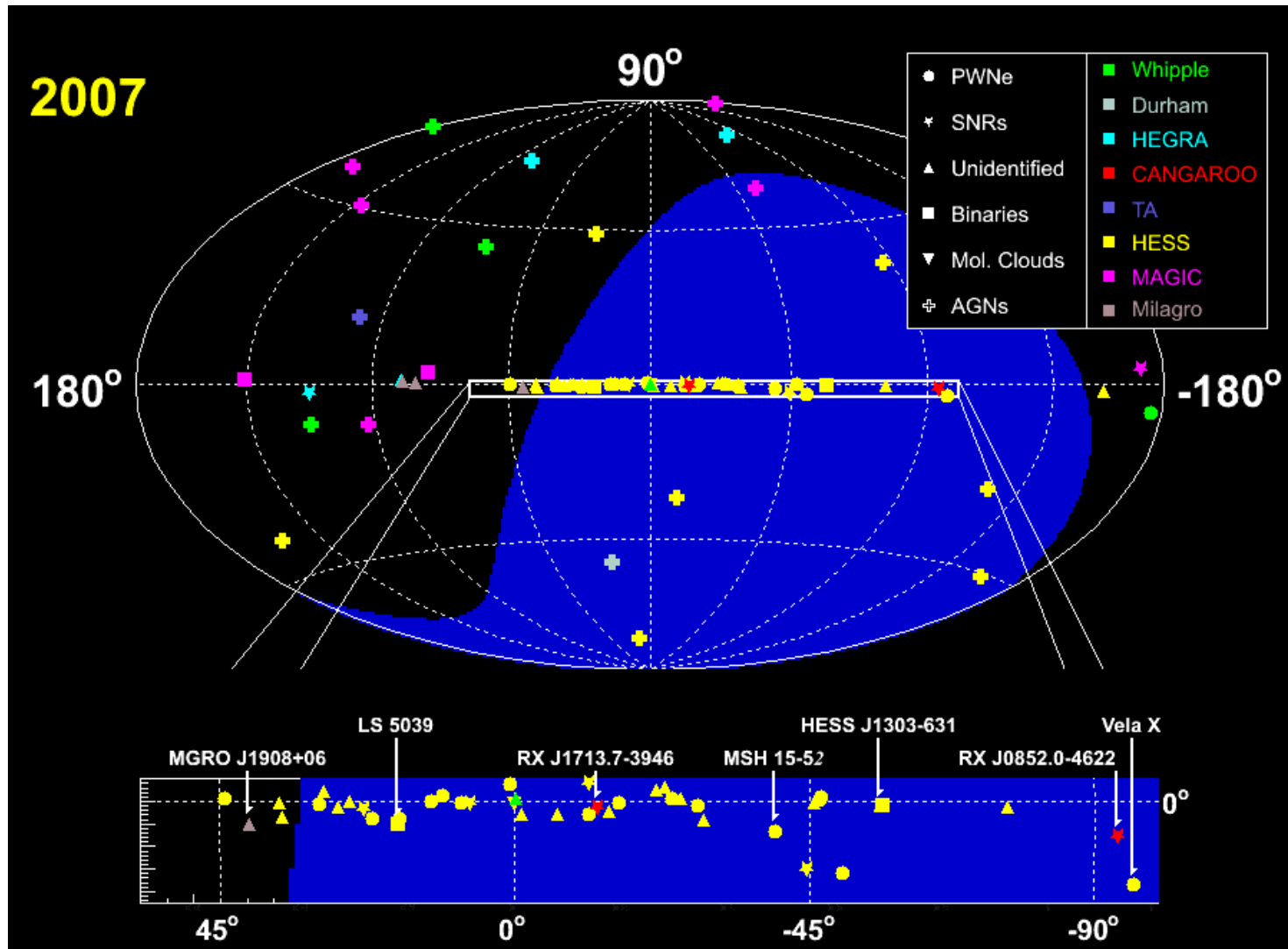
- 1171 WCDA (water Cherenkov for muon detection, 36m^2 , 30m spacing)
- 5195 surface scintillator detectors (1m^2 , 15 m spacing)
- 12 air Cherenkov telescopes



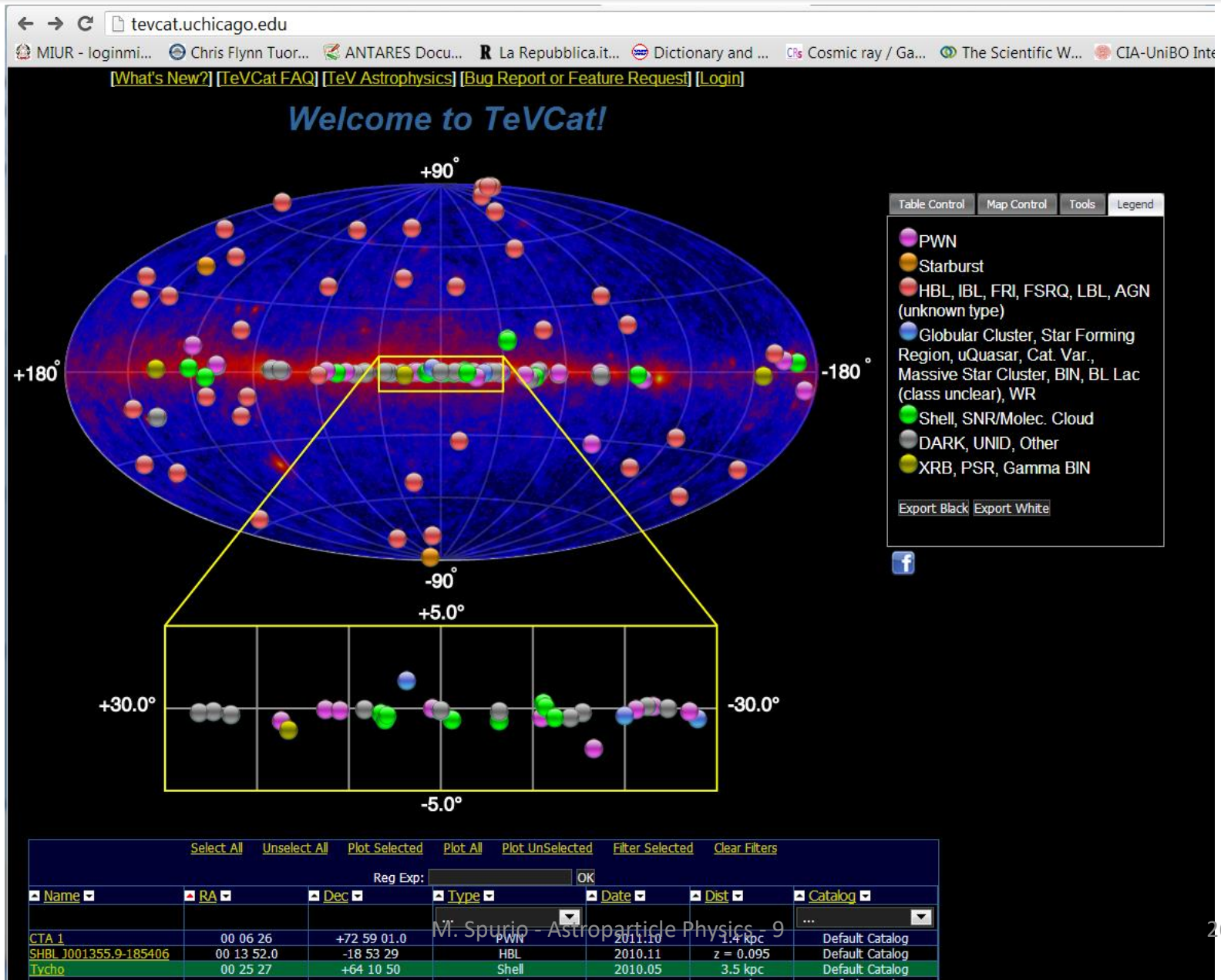
List of TeV sources in 2001



List of TeV sources in 2007



TeV sky today (2022) → 251 sources



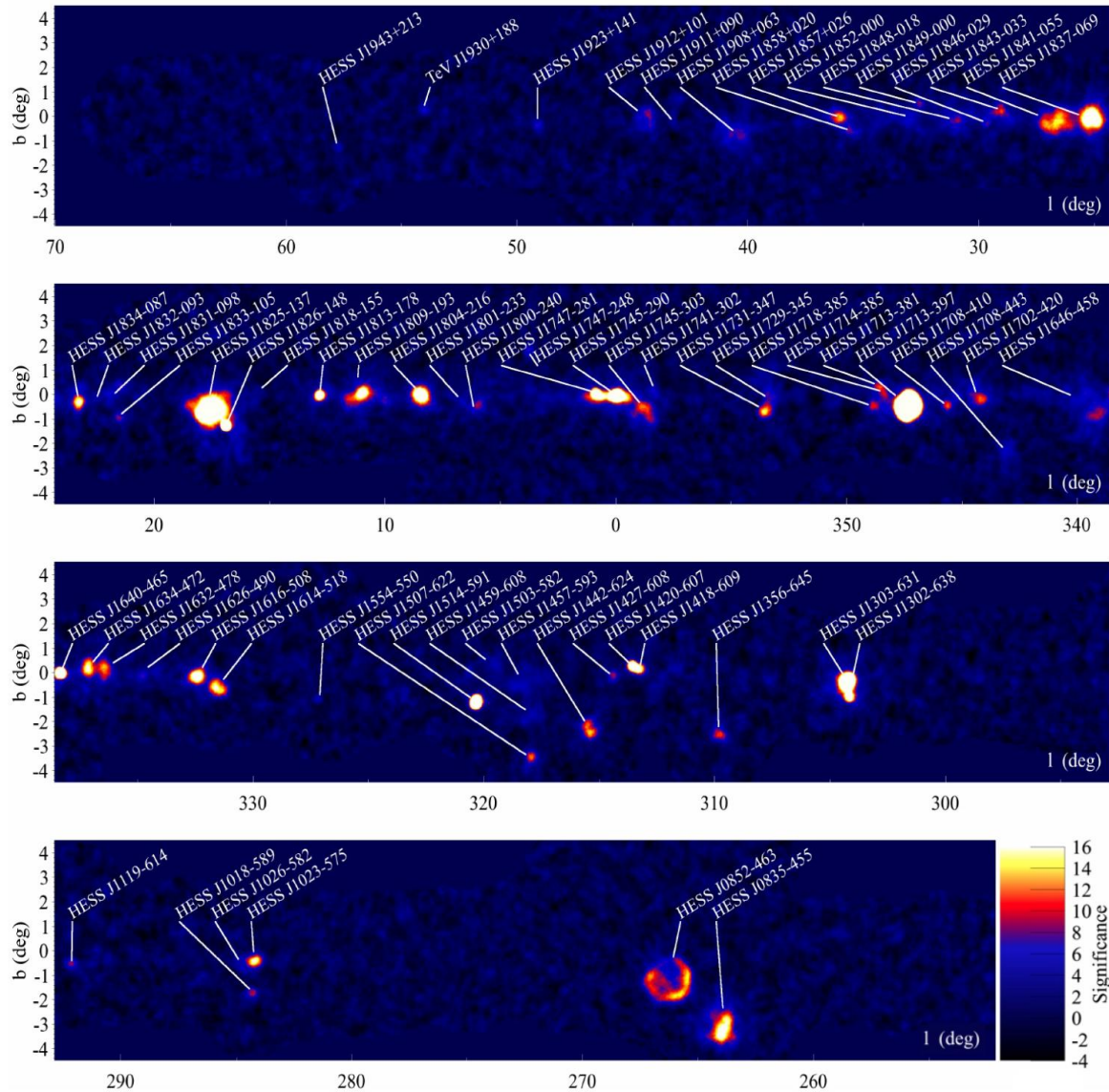
Type of TeV sources

- The wide FoV and the survey mode operation of LAT yield a roughly (within a factor two) uniform exposure to the entire sky.
- The IACTs have very narrow effective FoV and small duty cycle (10-15%): this means that each source must be individually studied by IACTs
- The [galactic plane is the only large fraction of the sky that has been studied](#) by HESS in detail with a dedicated survey of 2,800 ($-85^\circ < l < 60^\circ$; $-3.5^\circ < b < 3.5^\circ$): the survey has revealed more than fifty VHE γ -ray sources
- A large fraction (78%) of TeVCat Galactic sources corresponds to PWNe, located in close vicinity to young and energetic pulsars.
- Extragalactic sky is dominated by different AGN types

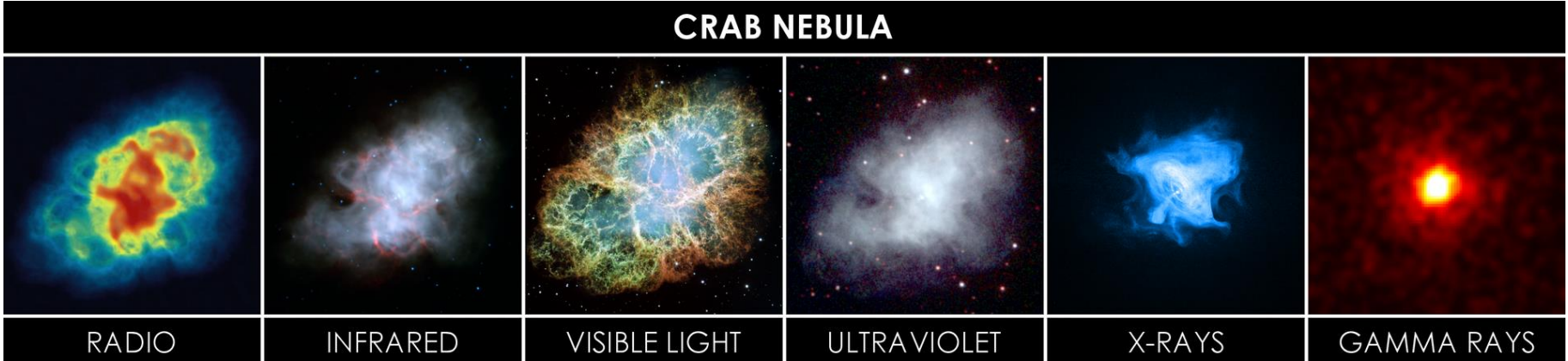
Total 251 sources

GRB	4	
No association	71	(0.29) [mostly Galactic]
Associated	176	(0.71)
Galactic	87	(0.495 associated -sources)
PWN/TeV-Halo/SNR	67	(0.78)
Binaries (Nova, Clusters,...)	11	(0.12)
Extragalactic	89	(0.505 associated sources)
AGN	87	
Starburst Galaxies	2	

The HESS survey of the galactic plane

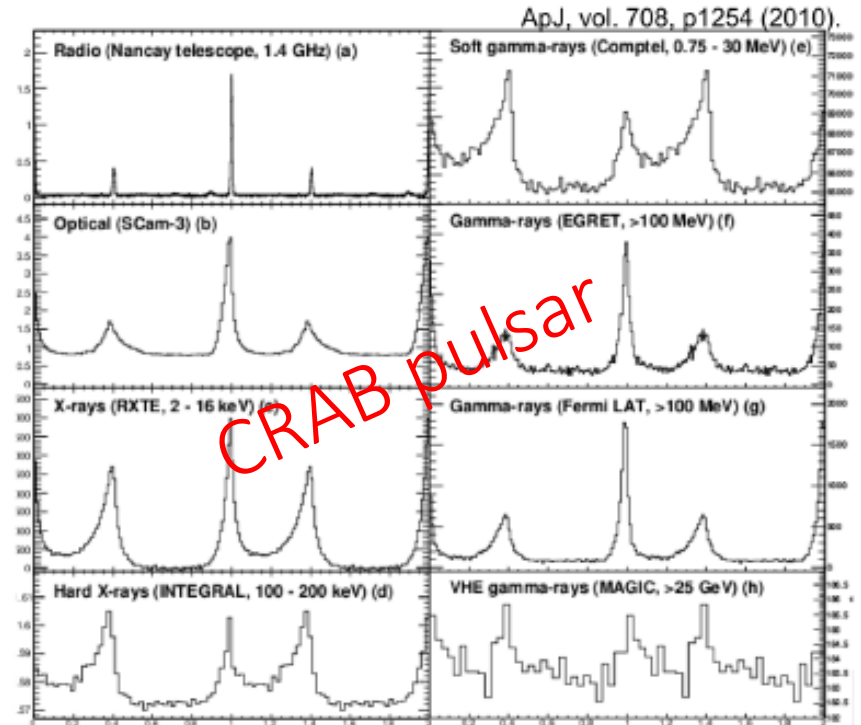


The reference source: the CRAB pulsar and nebula



Distance= (2.0 ± 0.2) kpc; Diameter=3.4 pc, apparent diameter of $7' \sim 0.1^\circ$; expanding at a rate of about 1,500 km/s, $v/c = 0.5\%$


- The Crab Pulsar and Nebula are a remnant of the supernova SN1054, which was widely observed on Earth in the year 1054.
- The Pulsar was discovered in 1968, and it was the first to be connected with a SNR.
- The Crab is the strongest TeV γ -ray source, and it is used as a gauge for other sources



The crab ($D=2.0\pm 0.5$) kpc

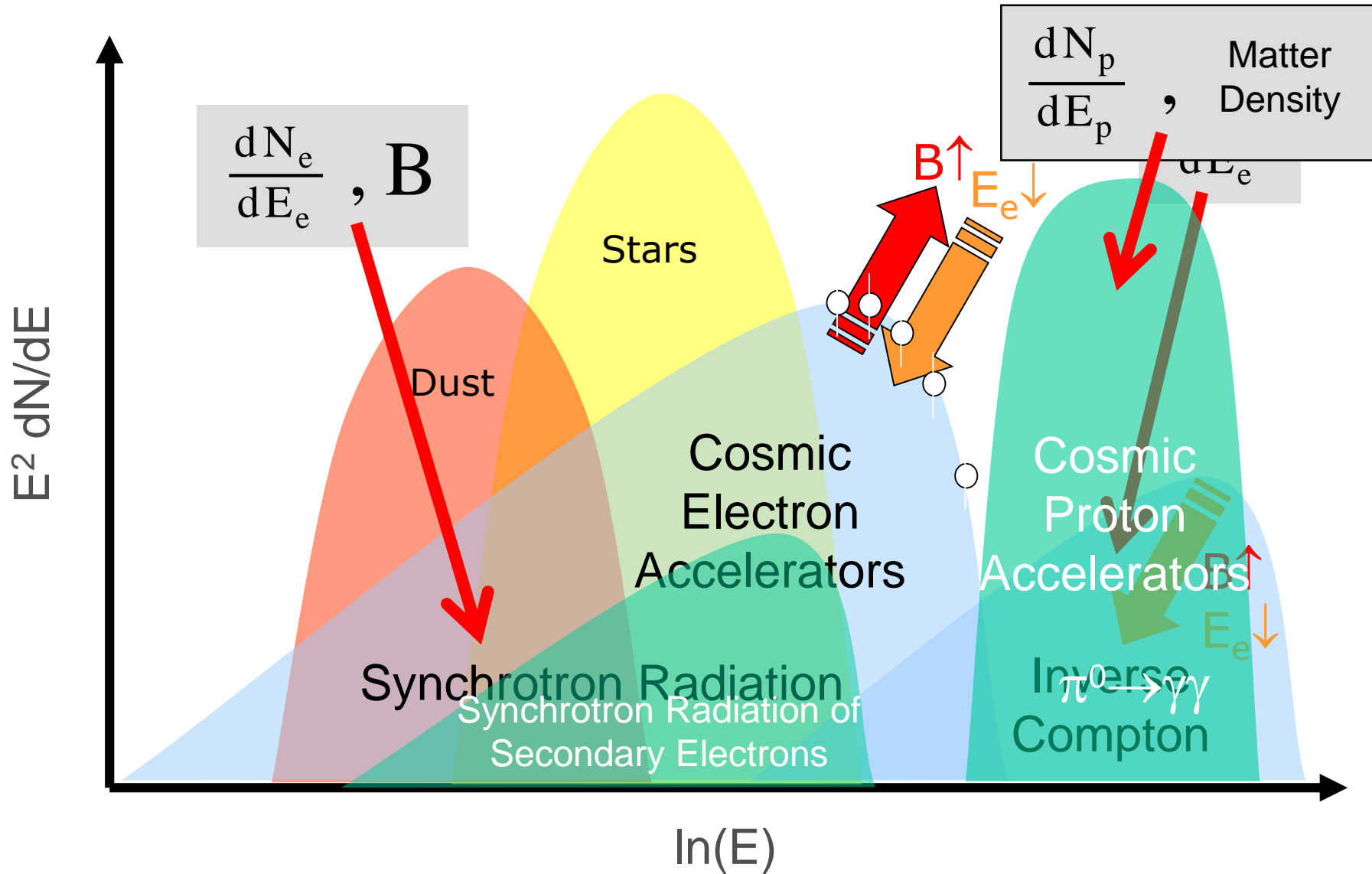
The CRAB Nebula

1 minute = 0.58 pc
= $1.8 * 10^{18}$ cm



6 arcminutes

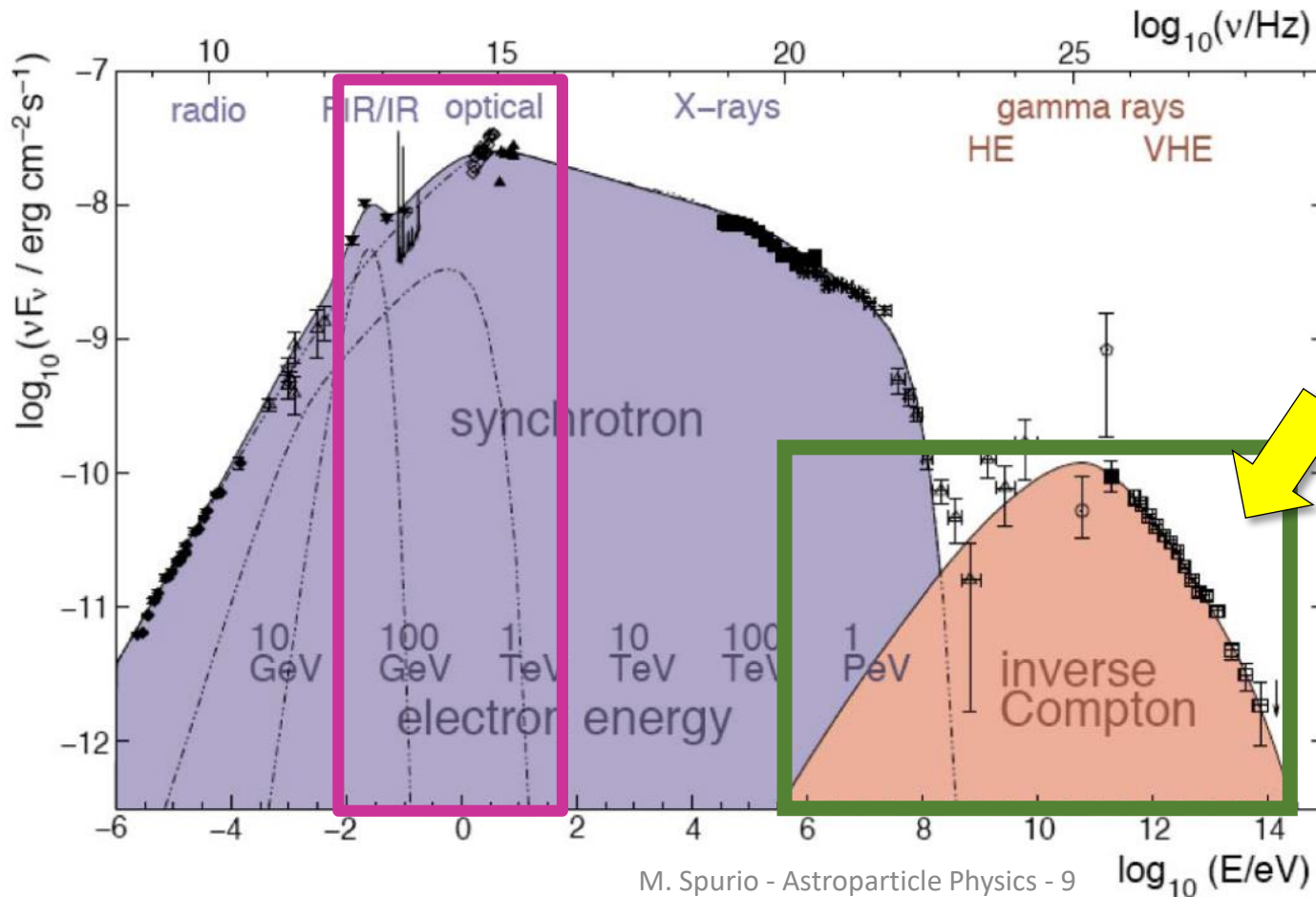
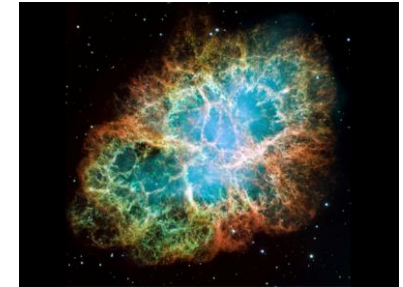
The Spectral Energy Distribution (SED)- [Chap. 8]



CRAB: a galactic source with leptonic emission



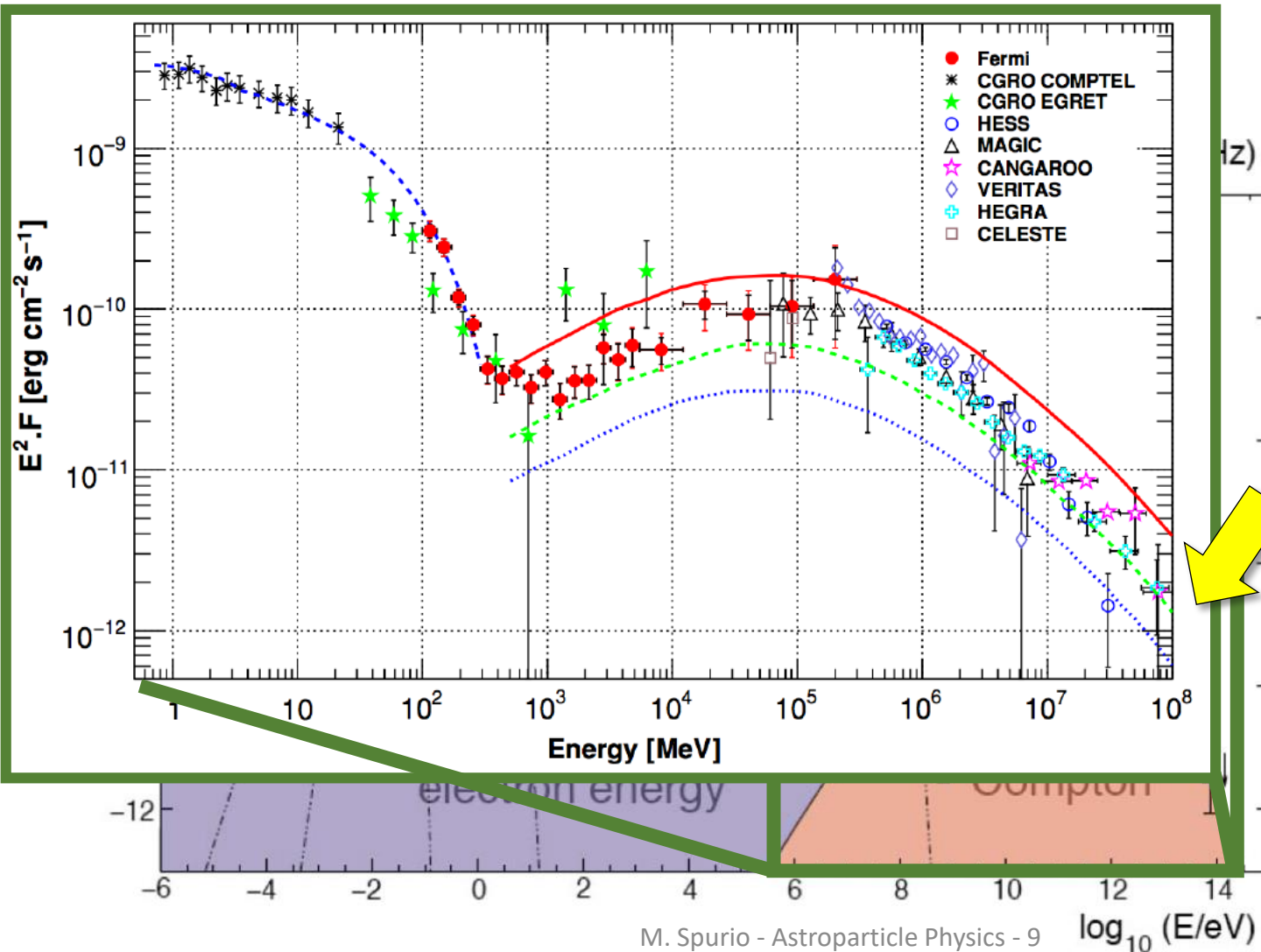
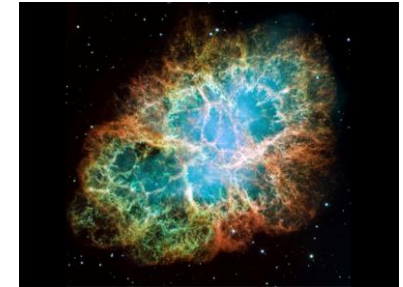
- A simple MHD model for the interaction of a HE electron-positron wind with the interstellar medium satisfactorily describes the main features of the non-thermal emission



- Figure represents the observed $E^2 \frac{dN}{dE}$ (SED) distribution from the Crab nebula.
- It extends over 21 decades of energies/frequencies.

CRAB: a galactic source with leptonic emission

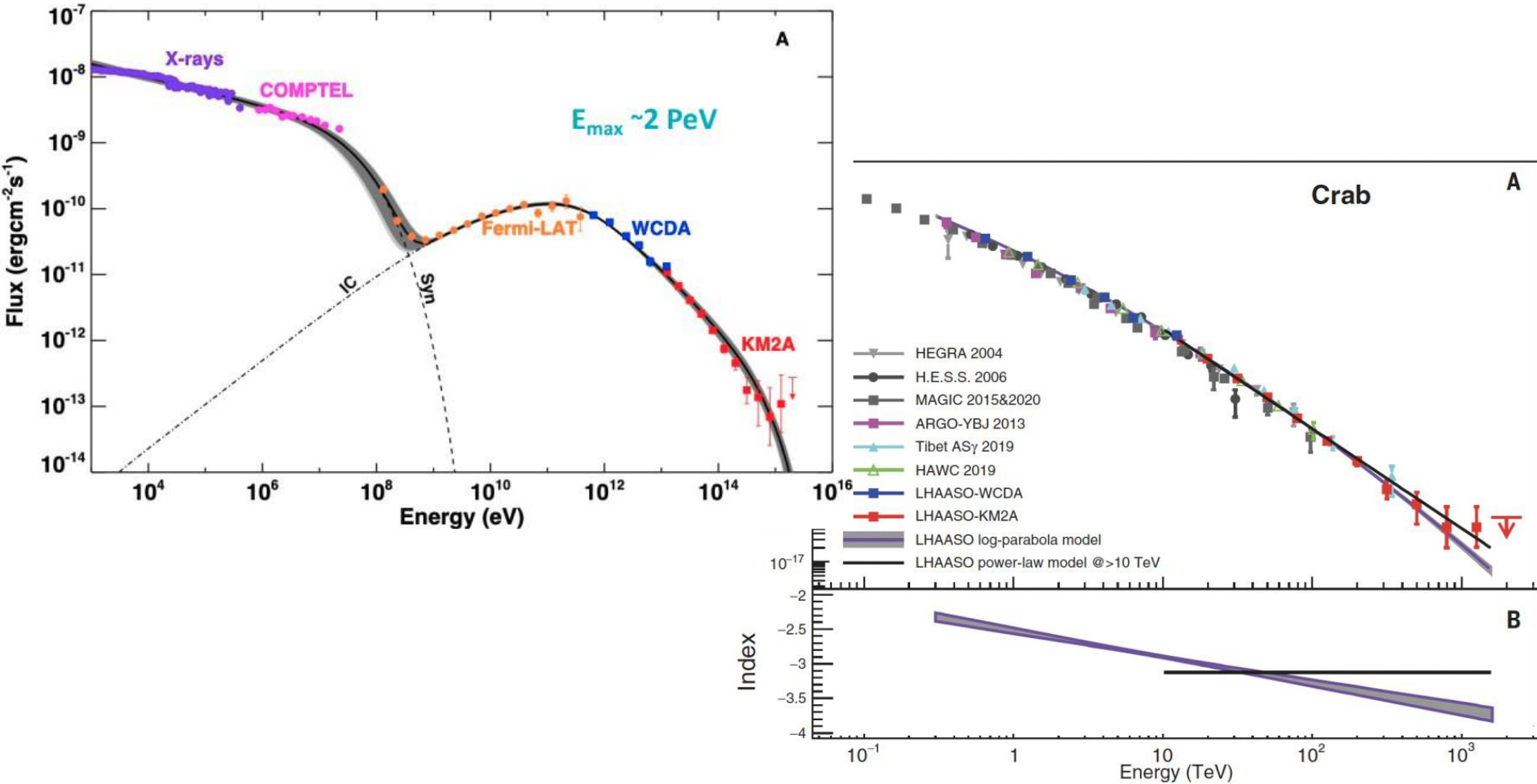
$$\mathcal{F}_\gamma(> 1 \text{ TeV}) = (2.1 \pm 0.1) \times 10^{-11} \frac{\text{photons}}{\text{cm}^2 \text{ s}}$$



- Figure represents the observed $E^2 \frac{dN}{dE}$ (SED) distribution from the Crab nebula.
- It extends over 21 decades of energies/frequencies.

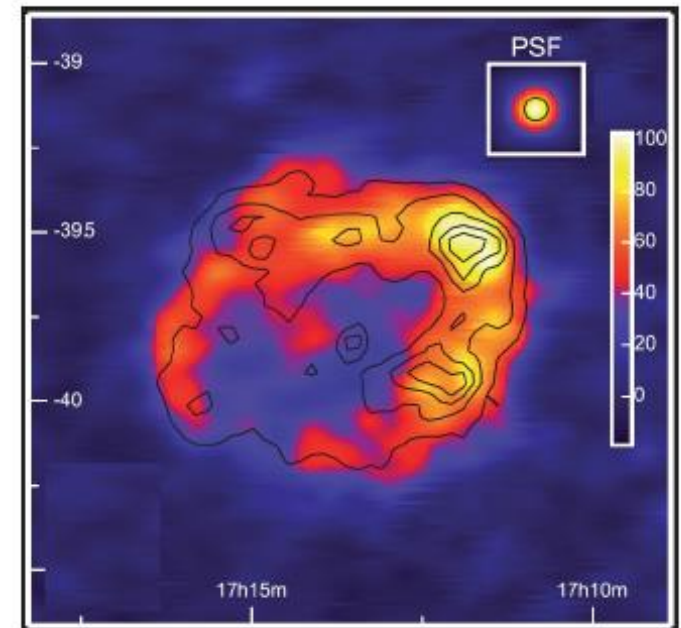
CRAB: a galactic source with leptonic emission

- Crab spectrum up to 1.1 PeV: electrons PeVatron
- 2.2 PeV electrons, challenging acceleration model



About the Identification of Galactic CR Sources

- The diffusive shock acceleration (DSA) model predicts the production CRs in SNRs;
- The amount of relativistic particles present in the acceleration region increases with time as the SNR passes through its free expansion phase, and reaches a maximum in the early stages of the so-called *Sedov phase* (Sect. 6.3.2).
- Correspondingly, the peak in γ -ray luminosity typically appears some 10^3 – 10^4 years after the supernova explosion.
- Thanks to the HESS survey of the galactic plane, we know that acceleration sites up to ~ 100 TeV are spatially superimposed with regions of non-thermal X-ray emission.
- This has strengthened the hypothesis that galactic CRs up to the knee are accelerated in SNRs.
- Figure shows the morphological structure of the RX J1713.7-3946 SNR. This shows a correlation of TeV emission with non-thermal X-rays.
- Even if radio and X-ray data suggest that SNRs are indeed the sources of CR electrons, **no compelling evidence for the acceleration of protons in SNRs up to the PeV energies has been found.**

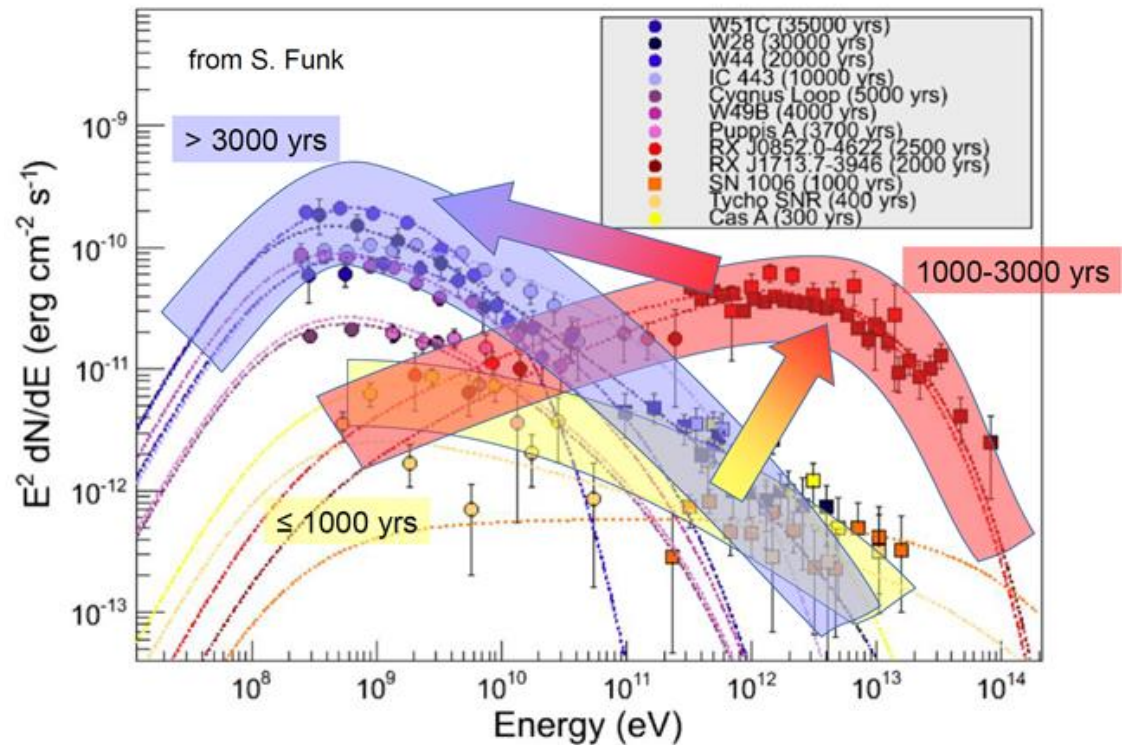


About the Identification of Galactic CR Sources

- A straightforward test of the acceleration of CRs in SNRs up to PeV energies would be the detection of γ -rays produced through the hadronic mechanism directly from young remnants and/or from dense clouds overtaken by the expanding shells.
- Multiwavelength observations are fundamental (and still not sufficient in most cases) to **disentangle leptonic or hadronic** mechanisms.
- Only the presence of HE neutrinos will be the proof of hadronic acceleration

- *The figure presents the SED of γ -rays from different SNRs at different ages. The largest energies are for SNe about 1-3 ky old.*

- *The Green catalog on radio observations contains 295 SNRs. Only 11 SNR have been firmly detected at TeV energies*



Example of spectral indexes: $\Gamma \sim 2$

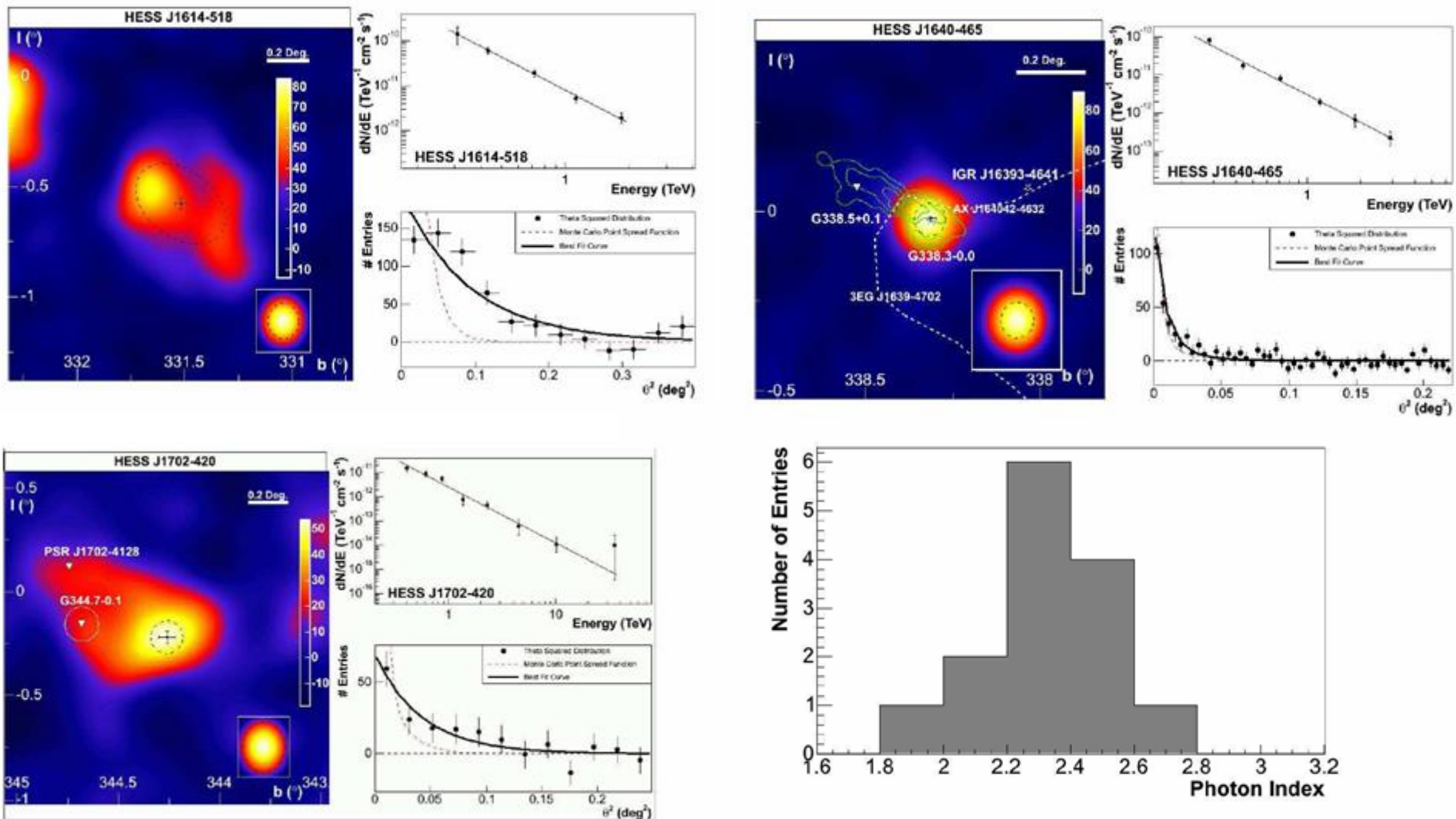


Fig. 8.— Distributions of the photon index of the new sources. The mean photon index is 2.32 with an RMS of 0.2.

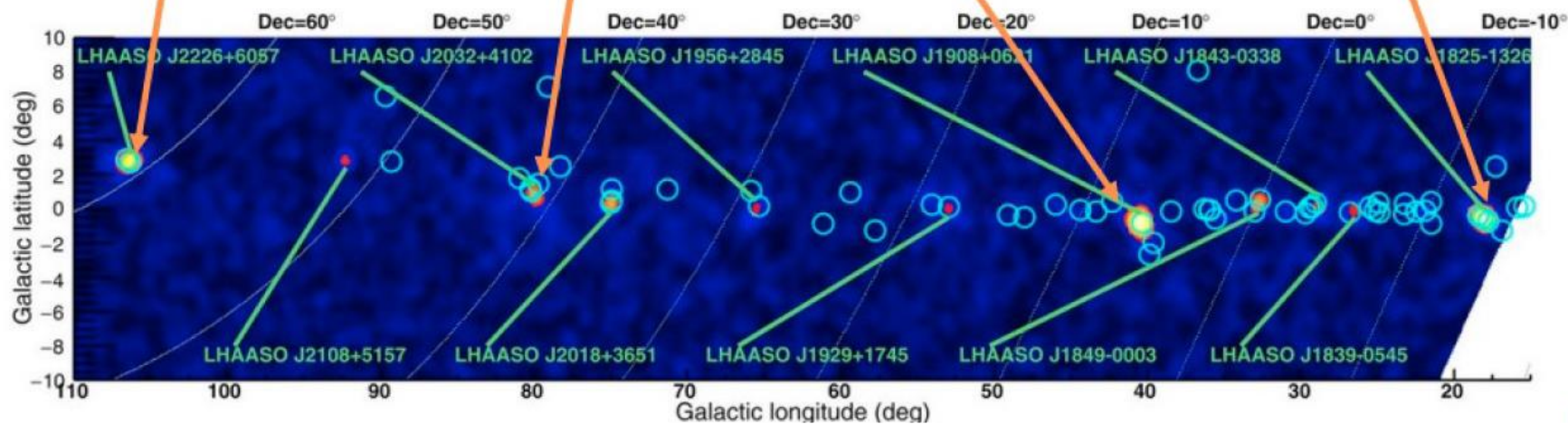
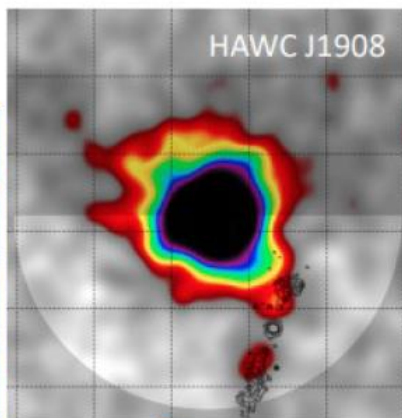
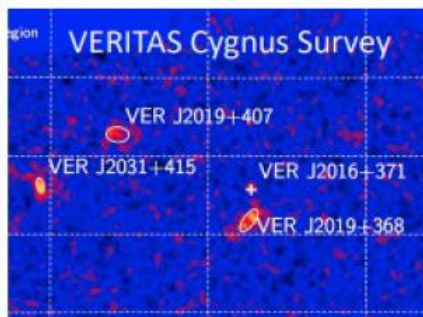
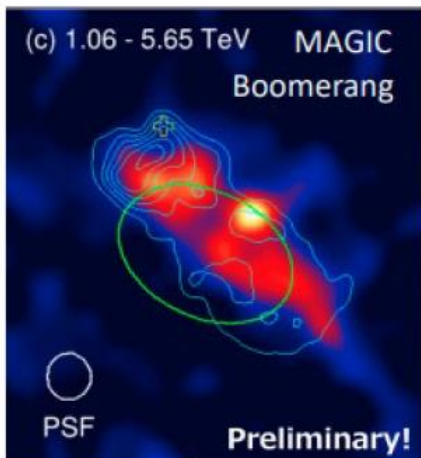
(2021) LHAASO first PeVatrons

Ultrahigh-energy photons up to 1.4 petaelectronvolts from 12 γ -ray Galactic sources

Zhen Cao , F. A. Ahnen

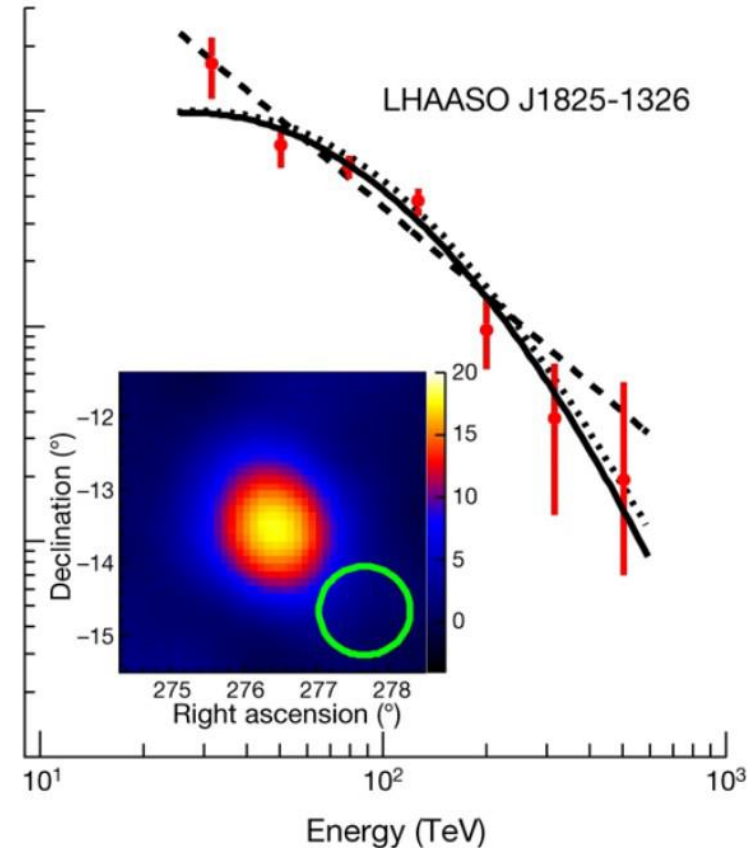
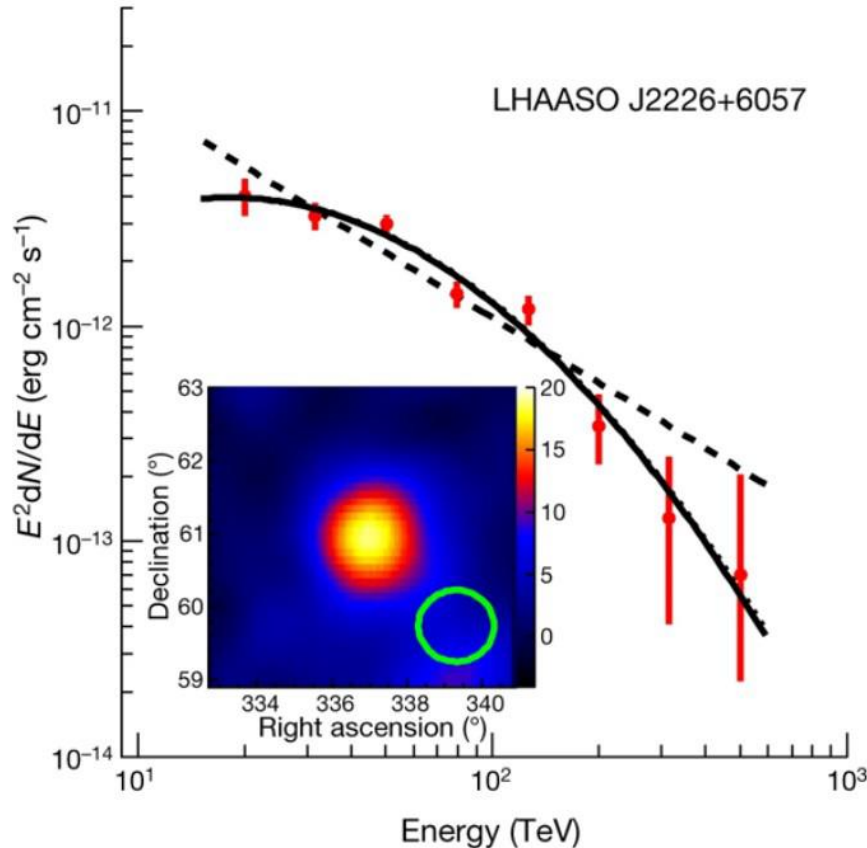
Nature 594, 33–36

- 1y, KM2A
- $E > 100 \text{ TeV}, > 7\sigma$
- Hadrons?



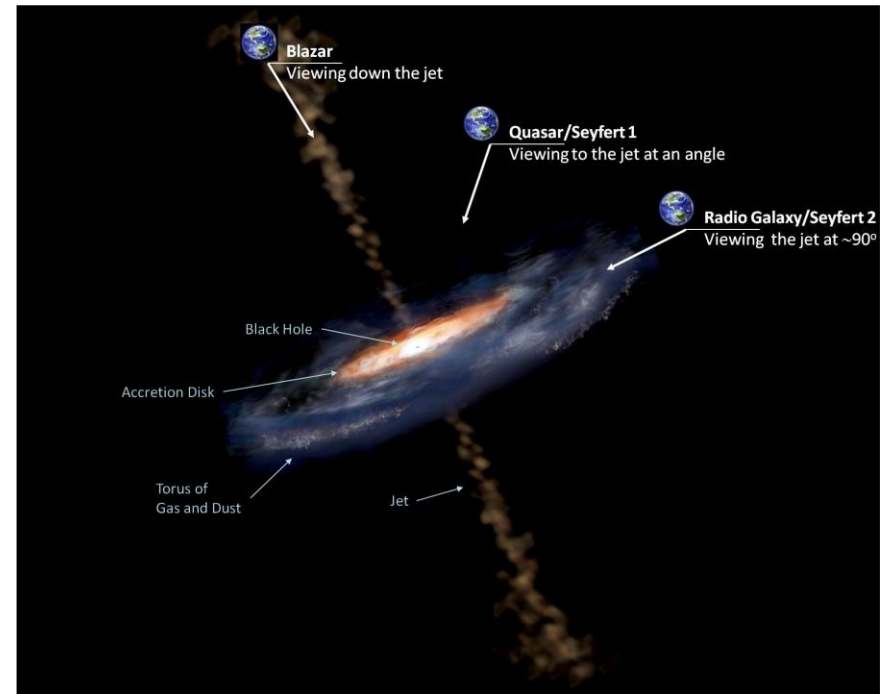
Hadronic PeVatrons ?

- Not yet demonstrated...but challenging for electrons
- To prove hadronic process:spectral signature:
 - neutral Pion bump vs IC/SSC
 - association with dense Molecular Clouds
 - smoking gun: neutrinos association



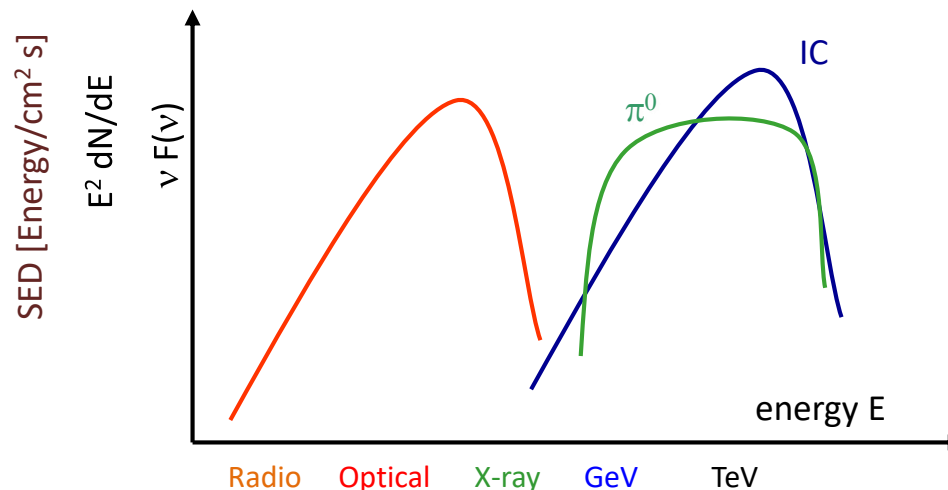
The extragalactic sky: AGN

- Active Galaxies are observed at different wavelength.
- Three main criteria are used to classify them:
 - (i) radio wavelengths yields a division into **radio loud and radio weak** objects;
 - (ii) The optical luminosity:
 - Radio weak sources are subdivided into **optically strong and optically weak**;
 - radio loud are subdivided in **low luminosity and high luminosity**;
 - (iii) The orientation of the AGN toward the observer.
- The radiation emitted is attributed to one of the two following processes:
 - *Thermal radiation*, from in-falling matter strongly heated in the accretion disk close to the central BH (**Seyferts galaxies, QSO**);
 - *Nonthermal emission*, by HE particles accelerated in a jet of material ejected from the nucleus at relativistic speed (*jet dominated AGN: Blazars, FSRQs, BL Lacs*)



The Spectral Energy Distributions of Blazars

- The study and classification of AGN and their acceleration mechanisms require observations from different instruments.
- The spectral energy distributions (SEDs) of blazars can span almost 20 orders of magnitude in energy, making simultaneous multiwavelength
- Usually, SEDs of different objects were obtained using data not collected at the same time. Only very recently strictly contemporaneous (or at least as contemporaneous as possible) and broadband sampling of SEDs been strengthened.
- This effort is particularly relevant for time-varying sources in which changes in overall brightness are often accompanied by changes in the energy spectra.
- One of the closer blazar is Mrk 421. The extensive multi-instrument (radio to TeV) data set provides an unprecedented, complete look of SED for this source.



SED for a normal/starburst galaxy

- NGC 7714 (a nearby starburst)
- NGC 6090 (normal galaxy)

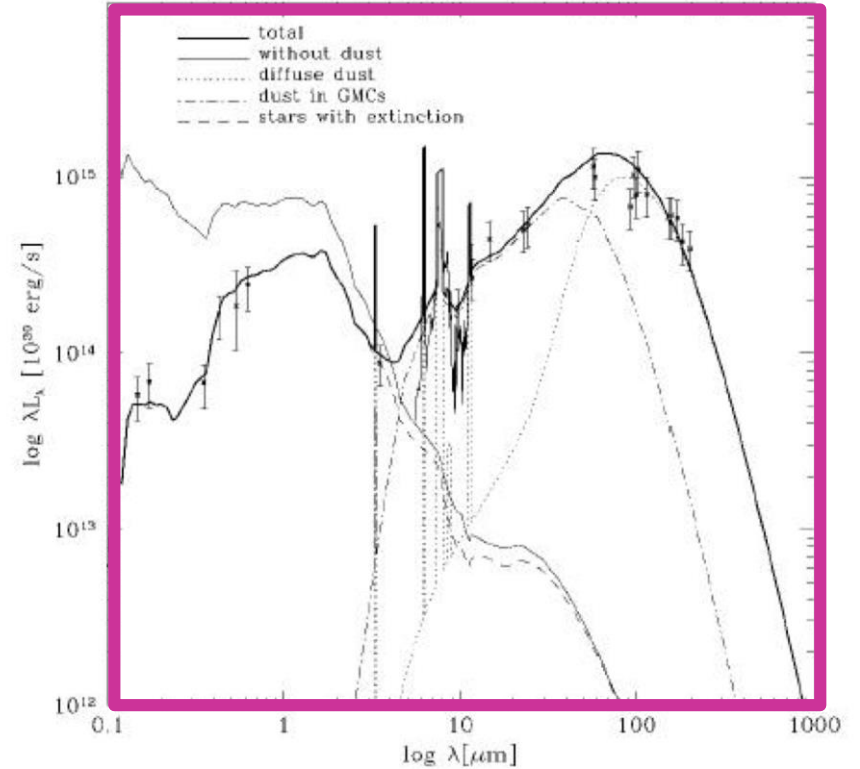
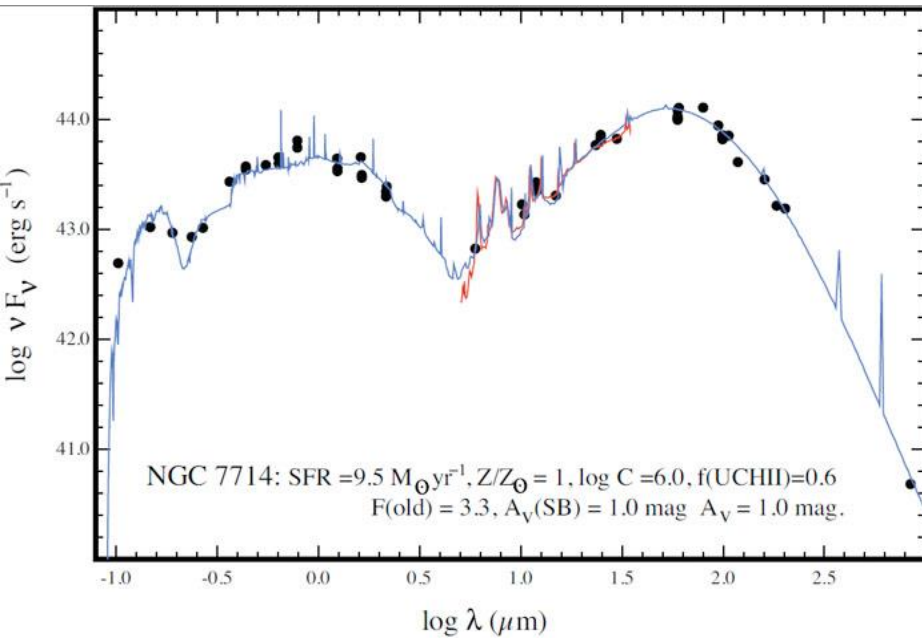
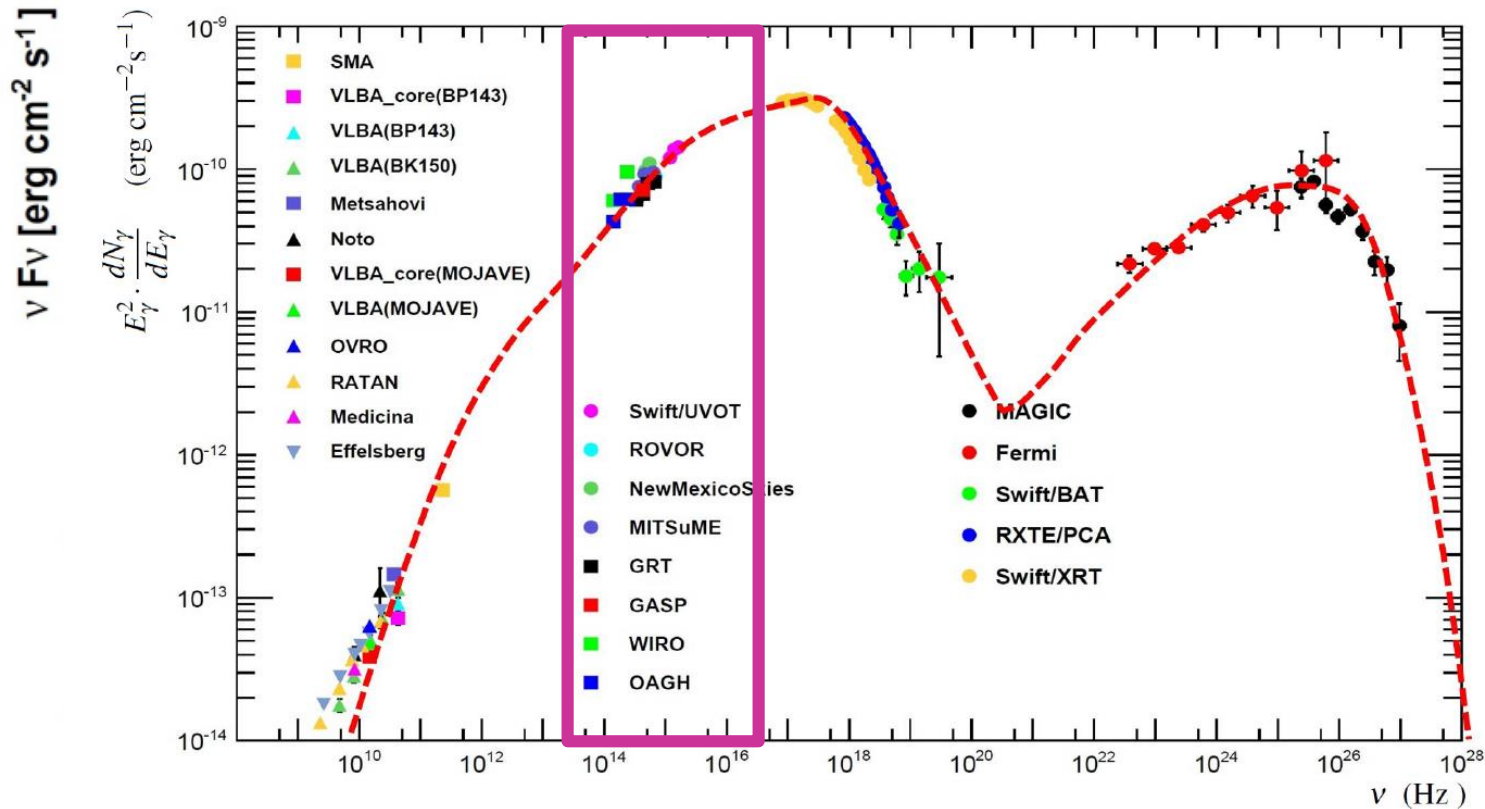


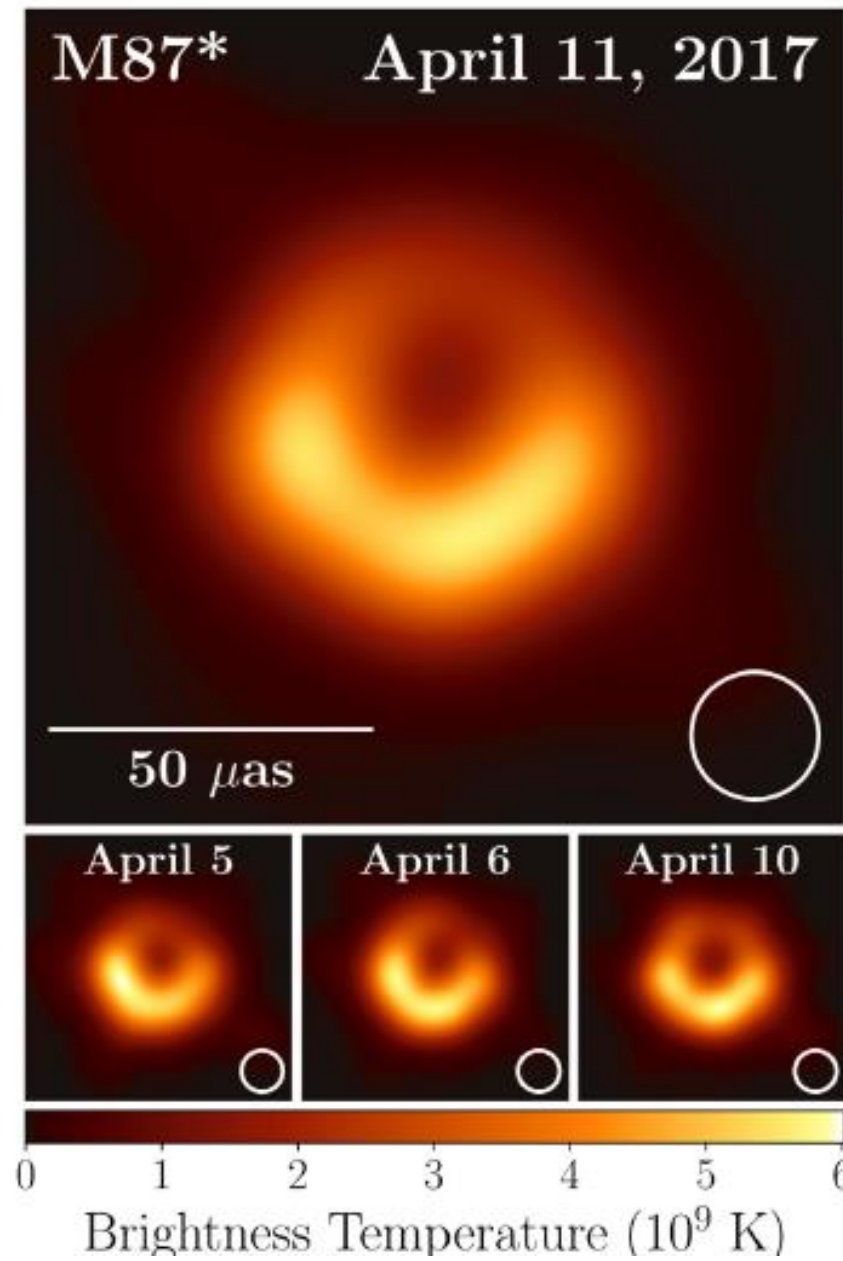
FIG. 8.—Fit to the SED of NGC 6090. Data are from Mazzarella & Boroson (1993), Acosta-Pulido et al. (1996), Gordon et al. (1997).

The SED of Mrk 421

Multiwavelength SED measurements (2009) of Markarian 421. The legend reports the correspondence between the instruments and the measured fluxes. The dashed line is a fit of the data with a **leptonic** model.



The central BH in M87



Event Horizon Telescope
10 April 2019
1st Image of a Black Hole

diameter = $42 \pm 3 \mu\text{as}$

Schwarzschild radius

$$R_S = \frac{2G}{c^2} M$$

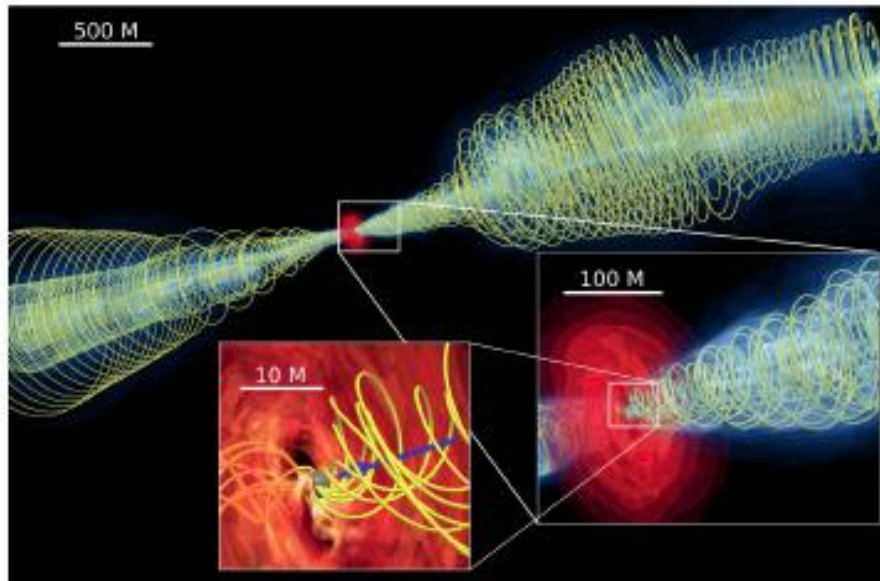
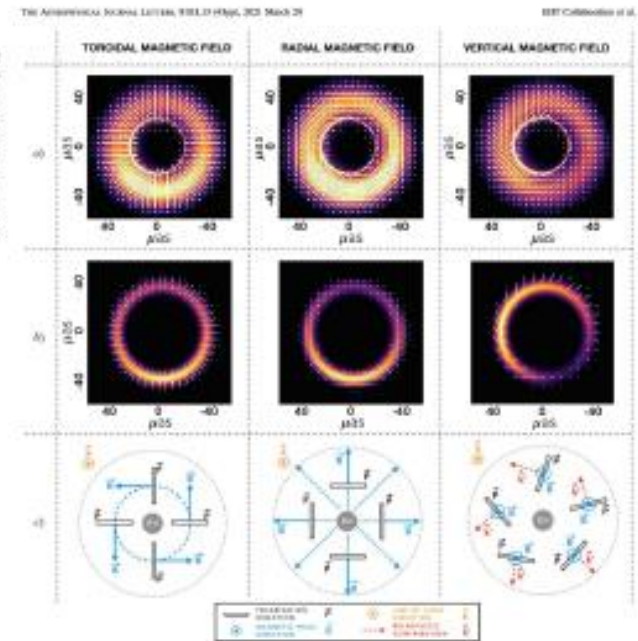
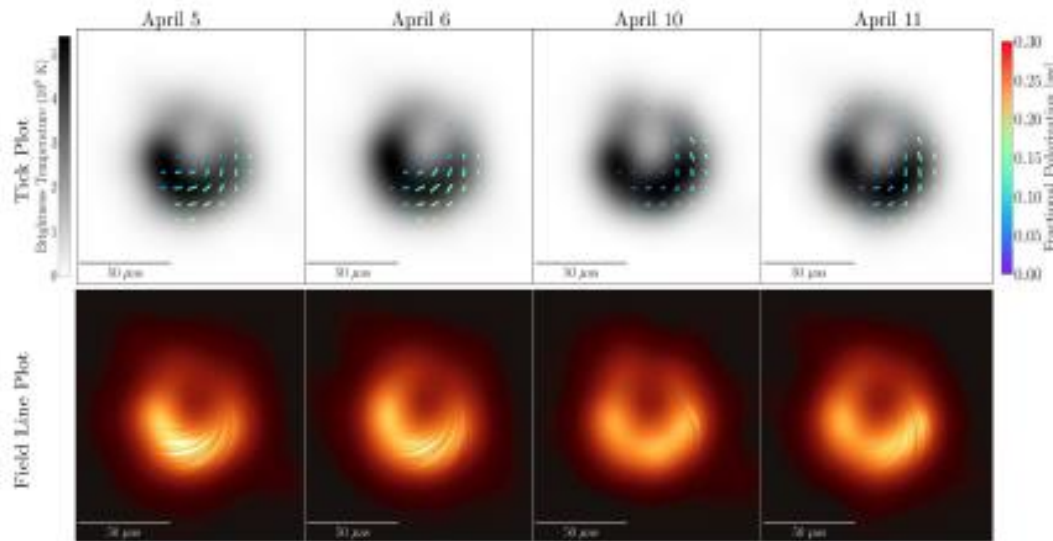
Photon capture radius

$$R_c = \sqrt{27} \frac{G}{c^2} M$$

$d = 16.8 \pm 0.8$ Mpc

$$M = (6.5 \pm 0.7) \times 10^9 M_\odot$$

Testing the jet formation



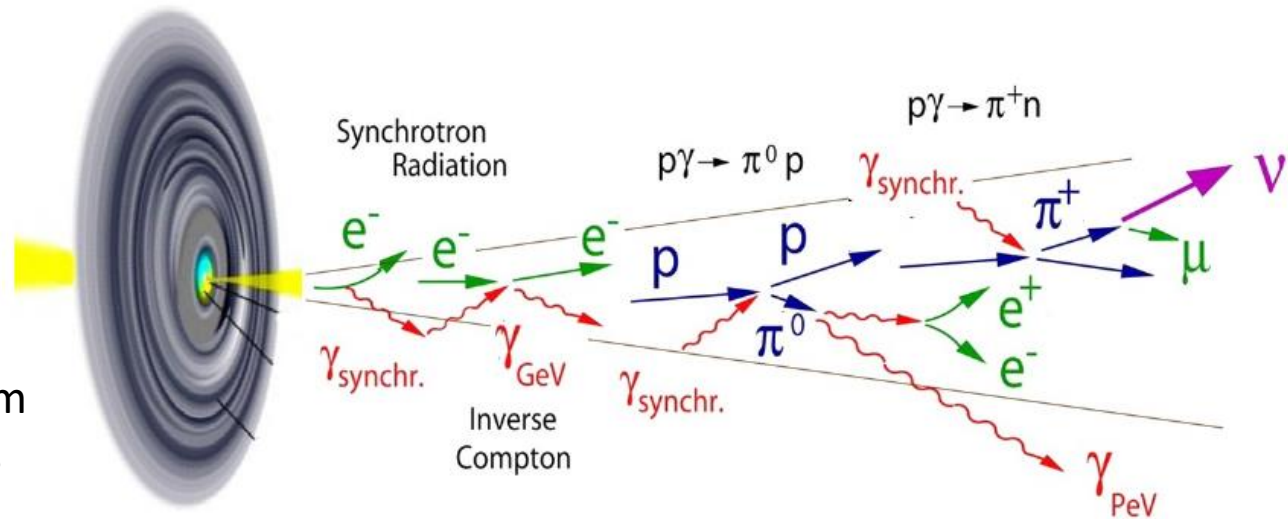
Reconstruction of magnetic field structure

A. Cruz-Osorio, *et al.*

“State-of-the-art energetic and morphological modelling of the launching site of the M87 jet”,
Nature Astron. **6**, no.1, 103-108 (2022)
 [arXiv:2111.02517 [astro-ph.HE]].

Jets in astrophysics

- Powerful relativistic outflows and jets, have been observed in different sources, as AGN and galactic objects such as pulsars and microquasars.
- If these outflows point toward us, as in blazars, relativistic effects can significantly change their appearance.
- The dynamics of nonthermal processes in these jets are important fields of research.
- The jet compositions and their production mechanisms are not completely understood.
- In AGN, models predict that the matter in the disk falls into the BH, converting a large fraction of the gravitational potential into kinetic energy.
- In some cases, particles in jet moves with relativistic bulk velocity (measured in the radio) up to Lorentz factors $\Gamma=50$ and with an extension that goes from fractions of kilo-parsecs up to hundreds of kpc.



The maximum EM luminosity

- Electromagnetic radiation can be produced from different emission mechanisms.
- In microquasars (§6.7.2), AGN (§9.9) and GRBs (§8.9), the energy production occurs by conversion of gravitational potential energy through accretion mechanisms.
- In the case a limit, referred to as the Eddington luminosity (or limit), exists.
- The Eddington limit gives the maximum luminosity that an astrophysical object can achieve. It is not possible to generate arbitrarily large luminosities by allowing matter to fall at a sufficiently great rate onto a black hole.
- If the luminosity is too large, radiation pressure would blow away the infalling matter. The limiting luminosity can be determined using hydrostatic equilibrium between the inward gravity force and the outward radiation pressure force.
- **EXERCISE: Derive the expression for the Eddington luminosity**

$$L_{\gamma}^E = 1.3 \times 10^{38} \left(\frac{M}{M_{\odot}} \right) \text{ erg/s .}$$

- **Solution: see “Extras” material of the book**
- The above holds for spherically symmetric phenomena. For a $10^9 M$ black hole, the corresponding Eddington limit is 2×10^{47} erg/s. It is possible to exceed that limit by adopting different geometries for the source region, but not by a large factor.

The Extragalactic Background Light

SKIP

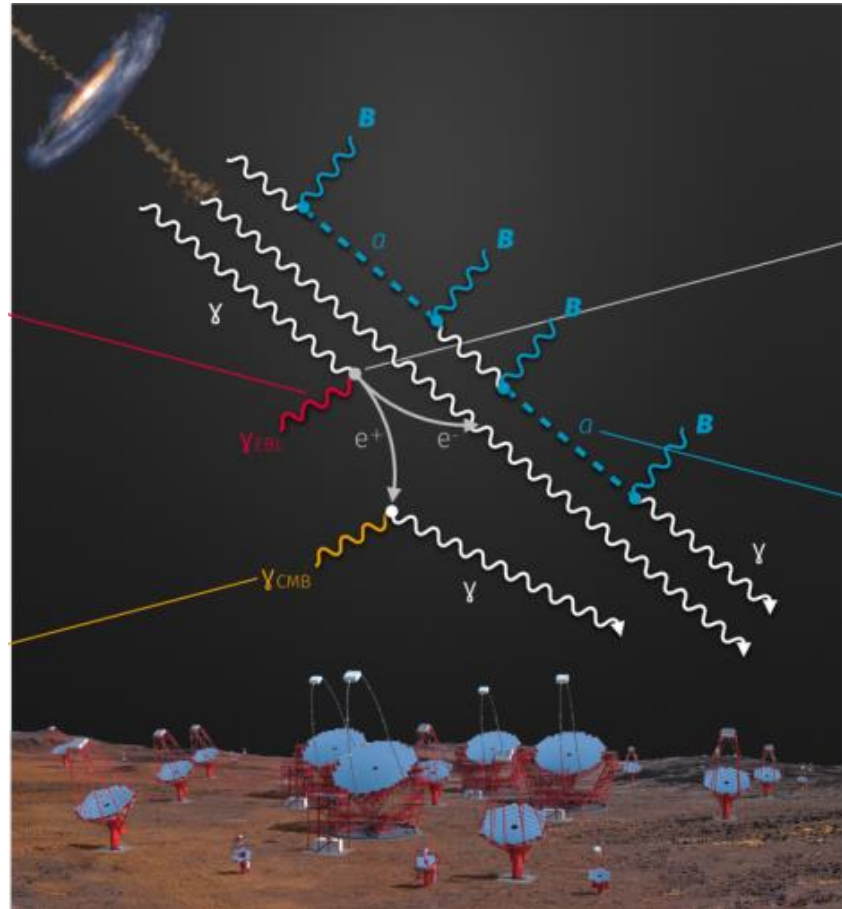
- The detection of γ -ray emitting blazars has started providing information useful for observational cosmology as well.
- The Universe is opaque to g-rays because of pair-creation processes

$$\gamma_E + \gamma_\epsilon \rightarrow e^+ e^-$$

Exercise:

- Estimate the average energy E for which the cross-section of the above process has a maximal on CMB.
- Show that for photons in the TeV range, the dominant process is on infrared/optical photons (**EBL**).

Solution: $E_{\gamma_{HE}} \cdot E_{\gamma_{cmb}} = (m_e)^2$

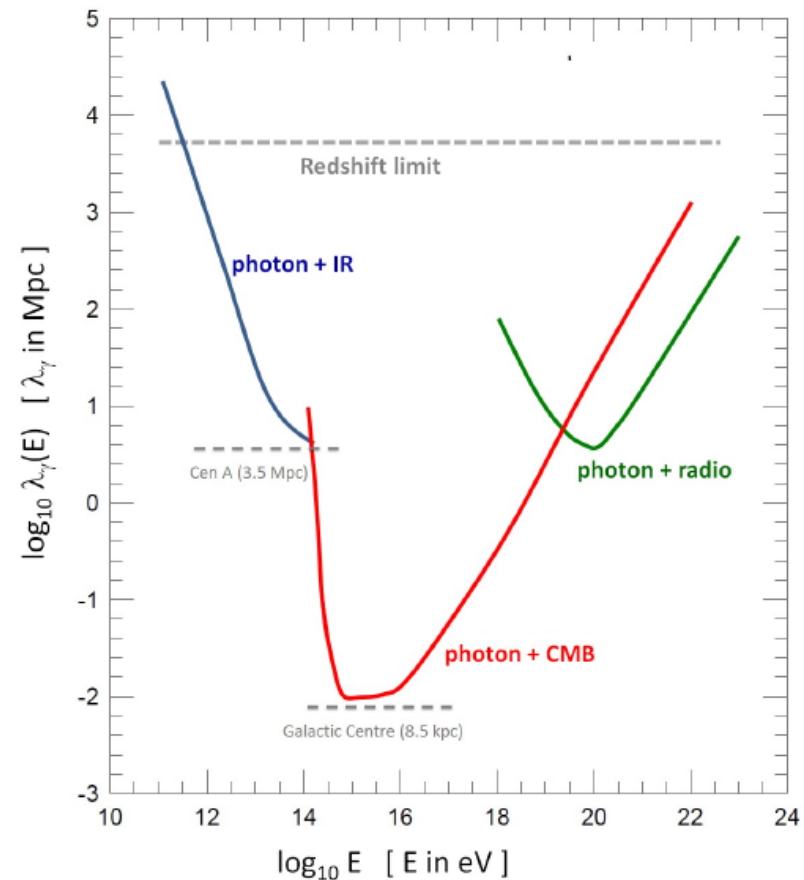


The γ -ray attenuation of the Universe

- The EBL is the totality of light emitted by stars, galaxies, and AGN over the lifetime of the Universe, modified by the redshift due to the expansion of the Universe.
- Therefore, in principle, the EBL contains information about the evolution of the baryonic components of galaxies and the structure of the Universe.
- Models for EBL are very poorly constrained.
- Once the energy density of the EBL has been assumed from a particular model, the optical depth $\tau(E; z)$ for a photon of observed energy E produced in a source at redshift z can be calculated.
- The attenuation of the γ -ray of energy E from the source at redshift z is

$$I(E, z) = I_0 e^{-\tau_{\gamma\gamma}(E, z)}$$

Figure shows the mean free path (in Mpc) of photons vs energy. Galactic sources start to be attenuated at >100 TeV by the presence of CMB. Photons from the nearby Universe (below some tens of Mpc) start to be attenuated above 10 TeV.



Left scale: SED per unit of solid angle for the extragalactic background light (EBL) energy density vs. E_γ (bottom scale) or λ (upper scale) for three values of redshifts. Right scale the energy density of the EBL

